2008

Quantifying Twentieth Century Glacier Change in the Sierra Nevada, California

Hassan J. Basagic
Portland State University

10.15760/etd.2236

THESIS APPROVAL

The abstract and thesis of Hassan Jules Basagic IV for the Master of Science in Geography were presented May 5, 2008, and accepted by the thesis committee and the department.

COMMITTEE APPROVALS:

[redacted]

Andrew G. Fountain, Chair

[redacted]

Keith S. Hadley

[redacted]

Martin D. Lafrenz

DEPARTMENT APPROVAL:

[redacted]

Martha A. Works, Chair
Department of Geography

ABSTRACT

An abstract of the thesis of Hassan Jules Basagic IV for the Master of Science in Geography presented May 5, 2008.

Title: Quantifying Twentieth Century Glacier Change in the Sierra Nevada, California

Numerous small alpine glaciers occupy the high elevation regions of the central and southern Sierra Nevada, California. These glaciers change size in response to variations in climate and are therefore important indicators of climate change. An inventory based on USGS topographic maps (1:24,000) revealed 1719 glaciers and perennial snow and ice features for a total area of 39.15 ±7.52 km^2. The number of 'true' glaciers, versus non-moving ice, is estimated to be 118, covering 15.87 ± 1.69 km^2. All glaciers were located on north to northeast aspects, at elevations >3000 m. Historical photographs, geologic evidence, and field mapping were used to determine the magnitude of area loss over the past century at 14 glaciers. These glaciers decreased in area by 31% to 78%, averaging 55%. The rate of area change was determined for multiple time periods for a subset of seven glaciers. Rapid retreat occurred over the first half of the twentieth century beginning in the 1920s in response to warm/dry conditions and continued through the mid-1970s. Recession ceased during the early 1980s, when some glaciers advanced. Since the 1980s each of the seven study glaciers resumed retreat.

The uniform timing of changes in area amongst study glaciers suggests a response to regional climate, while the magnitude of change is influenced by local topographic effects. Glacier area changes correlate with changes in spring and summer air temperatures. Winter precipitation is statistically unrelated to changes in glacier area. Headwall cliffs above the glaciers alter the glacier responses by reducing incoming shortwave radiation and enhancing snow accumulation via avalanching.

QUANTIFYING TWENTIETH CENTURY GLACIER CHANGE IN THE SIERRA NEVADA, CALIFORNIA

by

HASSAN JULES BASAGIC IV

A thesis submitted in partial fulfillment of the
requirements for the degree of

MASTER OF SCIENCE
in
GEOGRAPHY

Portland State University
2008

ACKNOWLEDGMENTS

I would like to thank my advisor, Andrew G. Fountain, for his support and guidance during this research, and my committee members, Keith S. Hadley and Martin D. Lafrenz, for their valuable insights.

I would like to acknowledge staff at Sequoia & Kings Canyon National Parks (SEKI) for their help, including Pat Lineback, Sylvia Haultain, Tony Caprio, Nate Stephenson (USGS BRD), and Hal Pranger at the Geologic Resources Division. I am especially grateful to Danny Boiano and Annie Esperanza for their help in developing this project and for their support and encouragement.

I appreciate the hard work provided in the field by Danny Boiano, Shane Fryer, Alysha Wilson, Ryan Branciforte, Jeff Kane, Jennifer Hook, and Rhonda Robb. Thanks for helping to carry heavy loads in difficult terrain. I would also like to thank archive staff who helped me locate photographs including Ward Eldredge (SEKI), Linda Eade (Yosemite NP), William Kerwin and Linda Reynolds (USFS Bishop). I thank Douglas Hardy for use of his Yosemite glacier photos. I benefited greatly from conversations with Keith Jackson, Matt Hoffman, and Peter Sniffen. Most importantly I thank my family for their support and encouragement throughout this process.

Support for this research came from the National Park Service, including Sequoia & Kings Canyon National Parks and the Geologic Resource Division, the National Science Foundation (BCS-0351004), and NASA (NNGO4GJ41G). I thank SEKI for their support through the Student Career Employee Program.

TABLE OF CONTENTS

SUPPLEMENTAL CD

Glacier inventory table

LIST OF TABLES

LIST OF FIGURES

1. INTRODUCTION

Alpine glaciers occur where snow accumulation exceeds loss. Because glaciers respond to changes in snowfall and air temperature they serve as an important indicator of climate change (Meier, 1965; Porter, 1981). Glacier mass change and subsequent retreat and advance are integrated responses to changes in climate (Hall and Fagre, 2003). Few climate records exist for alpine regions because they are remote and difficult to access, therefore knowledge of changes in glacier area, preserved by geological evidence, photographic records, and maps are important records of past climates. Over the 20^{th} century, with few exceptions, alpine glaciers have been receding throughout the world in response to a warming climate (Oerlemans, 2005). Globally, surface air temperatures have risen by $0.74° \pm 0.18°C$ over the past century (Trenberth et al., 2007), which has been the strongest warming trend in the past millennium (Jones et al., 2001). The shrinkage of alpine glaciers alters alpine hydrologic cycles and contributes to global sea level rise. Glaciers delay peak runoff from spring to summer, when less water is available and demand is high, modulating seasonal variations in runoff (Fountain and Tangborn, 1985). The shrinkage of glaciers reduces the ability of glaciers to delay runoff and buffer streams, resulting in earlier spring runoff and drier summer conditions. Alpine glaciers also release nutrients and regulate water temperatures which effect aquatic and riparian flora and fauna (Brittain and Milner, 2001; Dougall, 2007). The retreating alpine glaciers are estimated to account for 60% of the global sea level rise, at an estimated rate of 1.1 ± 0.24 mm yr^{-1} (Meier et al., 2007).

The magnitude of alpine glacier decline over the past century has been documented for many regions. In the European Alps, glacier area has decreased by 35% since 1850. New Zealand glacier area shrank by 49% during the same period (Hoelzle et al., 2007). In the western conterminous United States, glacier loss at Mount Rainier between 1910 and 1994 was 18.5% (Nylen, 2004), at Mount Hood between 1901 and 2004, 34% (Jackson and Fountain, 2007), at Glacier National Park, Montana 1850 to 1979, 65% (Key et al., 1998; Hall and Fagre, 2003), and in the Front Range, Colorado between 1916 and 2005, 40% (Hoffman et al., 2007).

A temporal pattern of glacier retreat –advance – retreat has emerged over the past century (Haeberli, 1995) since the end the Little Ice Age (LIA) (~1250 AD to ~1900 AD; Grove, 1988). Glaciers receded until the mid-20th century, advanced or stabilized in the 1950s - 1970s, after which glaciers generally retreated. While this pattern is global in extent, the magnitude and precise timing of loss has been spatially variable (Dyurgerov and Meier, 2000). Glaciers in the Western US, including those on Mount Rainer and Mount Hood, and in Glacier National Park followed this pattern. Glaciers retreated until the 1950s, advanced through the 1970s, and returned to retreat in the 1980s (Hall and Fagre, 2003; Nylen, 2004; Jackson and Fountain, 2007). Glaciers in the Colorado Front Range resumed retreat during the latter 1990s (Hoffman et al., 2007). Similarly, glaciers on Mount Shasta, California experienced fast retreat in the 1920s and 1930s after which they advanced through the second half of the century (Rhodes, 1987). Howat el al. (2007) report that two glaciers on Mount Shasta have advanced through 2003 as a result of enhanced precipitation. The difference in timing of glacier response highlights regional differences in high alpine climate. Consequently, it is important to examine various glacier regions to define local and regional climate variability.

Variations in regional climate are observed between glacier regions in the Western US, especially in precipitation. Spring snowpack records generally indicate decreases in April 1st snow water equivalent (SWE) over the past 50 years for the Pacific Northwest and Rocky Mountains, where as increases are reported at high elevation in the Sierra Nevada of California (Howat and Tulaczyk, 2005; Mote et al., 2005). Much of the variation in regional climate appears related to atmospheric patterns such as the Pacific Decadal Oscillation (PDO) and the El Niño Southern Oscillation (ENSO) in the Pacific Northwest and Southwest US (Mantua et al., 1997).

Glacier change in the Sierra Nevada has been largely overlooked. While knowledge of glacier shrinkage in the Sierra Nevada is common, there is little quantitative information on the magnitude or rate of reduction. The purpose of this thesis is to define the number and spatial extent of the Sierra Nevada glacier population using USGS topographic maps (1:24,000 scale), quantify the magnitude and rate of change in glacier extent for a small subset of glaciers, and compare the rates of change against climate variations. This thesis examines the glacier population and glacier change in two separate chapters followed by two analysis chapters that compare glacier area changes with climate and explore the topographic effects. on glacier change.

Conceptual framework

The link between climate change and glacier response is indirect. Meier (1965) defined the relationship between changes in glacier geometry and climate through a series of connected processes (Figure 1). The general or regional climate, modified by local conditions, determines the surface mass and energy exchanges that determine a glacier's mass. A change in mass produces a dynamic response that causes changes in glacier geometry. Observations of glacier geometry through time indicate changes in both regional climate and local climate of the glacier. I examine changes in glacier geometry in this thesis to infer changes in regional climate and then compare these results to variations in climate.

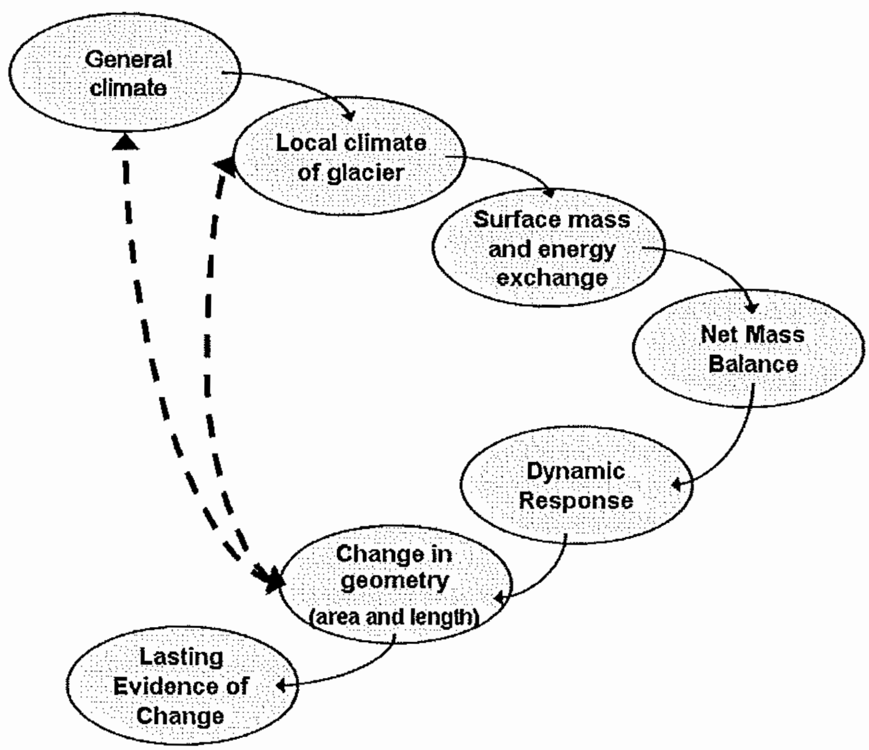

Figure 1. Processes linking climate and glacier area change. Larger dashed arrows indicate my approach to inferring climate change from glacier area changes and comparing the results to variations in climate (Meier, 1965; Fountain et al., 1997).

It is important to clearly define the term glacier. Glaciers are generally defined as masses of perennial snow or ice that move (Paterson, 1999). Here, I use a more inclusive term of 'glacier' that includes moving glaciers and stagnant perennial ice and snow patches. I differentiate between the two by referring to glaciers that move as 'true' glaciers and the others as perennial snow and ice.

2. STUDY AREA

The Sierra Nevada is situated along the eastern edge of the state of California (Figure 2). The mountain range stretches over 640 km from Tehachapi Pass northward to Lassen Peak, and varies in width from 65 to 130 km. The Sierra Nevada rise gradually above the Central Valley to the Sierra crest where elevations drop quickly into the high desert valleys of California and Nevada. The region has high relief ranging in elevations from 450 m in the western foothills to alpine peaks > 4000 m.

The climate in the Sierra Nevada is characterized by cold wet winters, and hot dry summers (NCDC, 2006). This climate is controlled by the migration of the Pacific High pressure system. In summer, the Pacific high moves north, off the California coast and deflects storms northward. Summer moisture comes from the Gulf of Mexico and Gulf of California, often resulting in localized thunderstorms. In winter, the Pacific High moves south, enhancing onshore flow and precipitation into the Sierra Nevada (Major, 1990). The Sierra Nevada is an effective barrier to westerly storms resulting in heavy snowfall at higher elevations and create a rain shadow to the east. The South Entrance Yosemite station on the western slope receives about four times the winter precipitation as the east side Lee Vining station (Figure 3).

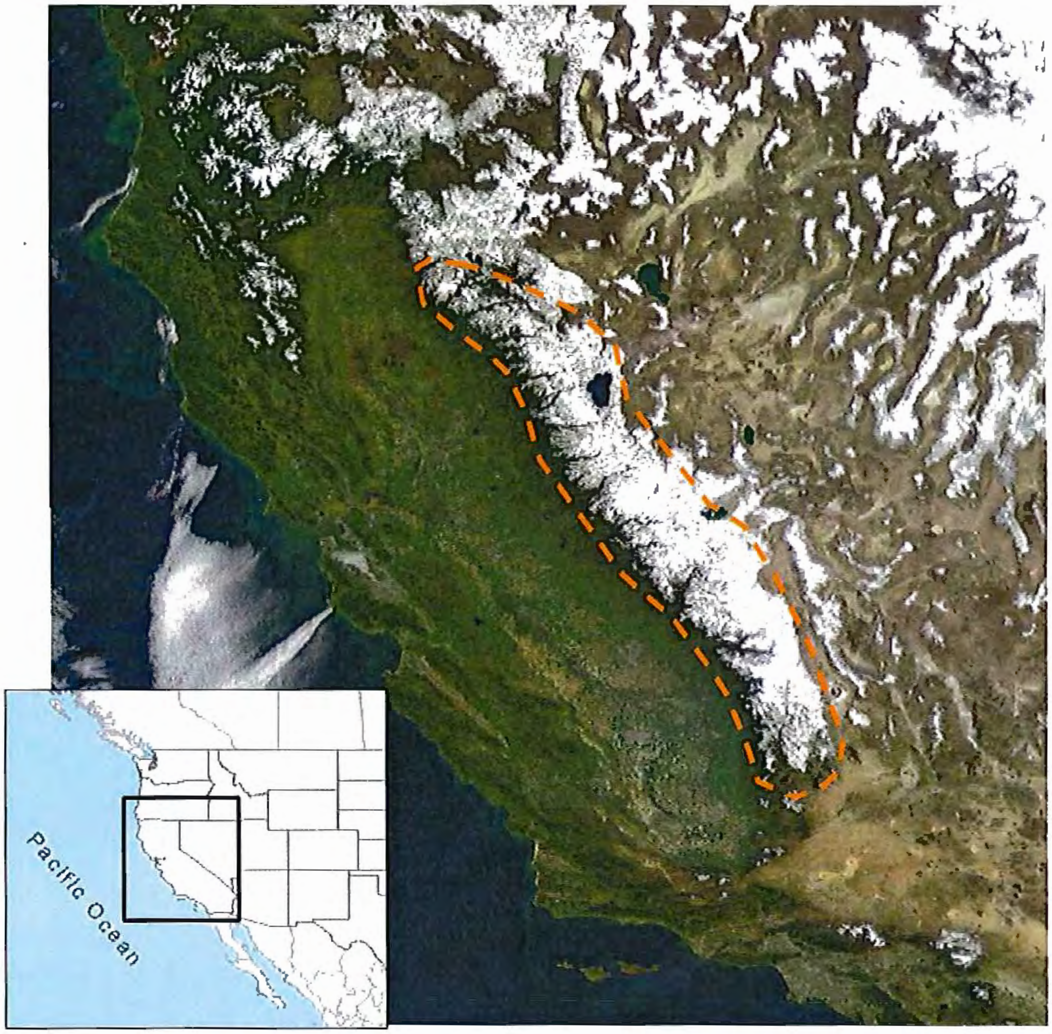

Figure 2. Image of the Sierra Nevada (dashed orange line) with fresh snow in high elevation areas (NASA MODIS image, March 3, 2004)

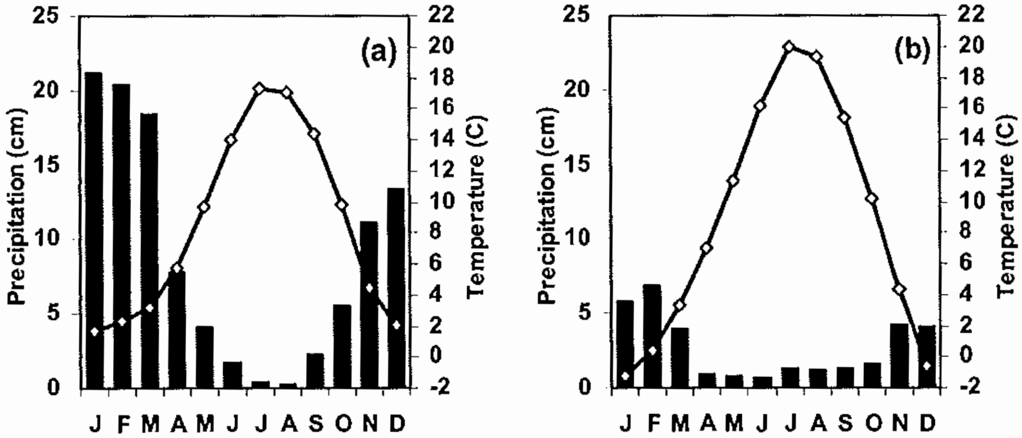

Figure 3. Monthly climate normals (1971-2000) for mean precipitation (bars) and mean temperature (circles) at two stations (NCDC, 2002): (a) Yosemite National Park South Entrance Station (1560m), and (b) Lee Vining (2073m).

The glacial history of the region is relatively well known. Geologic evidence indicates at least five major glacier advances during the Pleistocene (oldest to youngest): McGee, Sherwin, Tahoe, Tioga, and Recess Peak (Blackwelder, 1931; revised by Clark and Gillespie, 1997). Multiple glacier advances occurred throughout the late-Tahoe and Tioga periods with the Last Glacial Maximum occurring 21 ± 2 ka B.P. (Benson et al., 1996). The late-Pleistocene Recess Peak advance, was first suggested as late-Holocene (Birman, 1964), but evidence now indicates the advance occurred between 14.2 and 13.1 ka B.P. (Clark and Gillespie, 1997). Recess Peak glaciers were less extensive than the Tioga advance, with glaciers reaching lengths of about 2 km. Recent evidence from lake sediments indicate that following the Recess Peak advance, the Sierra Nevada may have been free of glaciers between 10.5 - 3.2 ka B.P., except between 5.4 and 4.8 ka B.P. (Bowerman, 2006). Following the onset of late-Holocene glaciation 3.2 ka B.P., distinct neo-glacial maxima occurred at ~2200,

~1600, ~700, and ~170-250 yr. B.P. (Bowerman, 2006). The most recent glacial advance was named the Matthes (Birman, 1964). Matthes (1939) first applied the name "Little Ice Age" to note the cool period with renewed glaciation beginning less than 4 ka B.P., based on lake sediment evidence from Owens Lake (Antevs, 1938). LIA generally refers to the cool period from A.D. 1250 – 1900 when glaciers advanced throughout the northern hemisphere (Grove, 1988). In the Sierra Nevada, the cool and moderately dry period is evident in lake sediments, tree-rings, and moraine records (Stine, 1996). The LIA glacial maximum occurred between 100 – 200 yrs B.P. (Clark and Gillespie, 1997). Photographic evidence from Russell (1885) shows several glaciers had slightly receded from their moraines in 1883, indicating that the maxima occurred before that time. Curry (1969) concluded that LIA reached a climatic maximum sometime between 1895 and 1897 based on dendrochronological records and historical glacier photographs.

Today, small alpine glaciers occupy high elevation mountain cirques in the central and southern Sierra Nevada (Figure 4). Typically, these glaciers occur on north and northeast aspects. Glaciers are located between 36.37° and 38.37° N latitude at elevations between 3090 and 4148 m (Raub et al., 2006).

Figure 4. Small alpine glaciers of the Sierra Nevada south of Mount Darwin.

Previous Glacier Studies

Glaciers in the Sierra Nevada were first noted by John Muir in 1871 when he proclaimed he had found "living glaciers" (Muir, 1873). Muir's report was preceded by the first published account of glaciers in the Western US by Clarence King on Mount Shasta (King, 1871). Muir confirmed active movement at Maclure and Lyell glaciers in 1872 by conducting velocity studies on glaciers with stake measurements (Muir, 1873). Joseph LeConte confirmed Muir's findings the following summer (LeConte, 1873).

An early USGS expedition headed by I.C. Russell produced the first glacier map in the Sierra Nevada and the first lithographs of Lyell and Dana glaciers (Russell, 1885). Russell observed multiple moraines during the expedition and suggested that multiple glaciations had occurred in the region in response to climate changes, and that the present glaciers were not remnants of the Pleistocene Ice Age (1889). Gilbert (1904) conducted the first glacier change study in the Sierra Nevada. Gilbert, who had accompanied Russell in 1883, rephotographed Lyell Glacier and compared his results to the 1883 Russell lithographs. Gilbert reported little change in the glacier and suggested monitoring the glaciers for future changes. Based on photographic evidence Curry (1969) suggested the glaciers retreated and then rapidly advanced to reoccupy their LIA moraine between the visits of Russell in 1883 and Gilbert in 1903. Gilbert returned to the Sierra in 1908 to photograph the glaciers establishing a valuable photographic record of Darwin and Goddard glaciers. Curry's photographic evidence (1969) indicates that glaciers remained at their maximum through 1907 and 1908. Early glacier change was first noted in 1919 at Lyell Glacier (Farquhar, 1920).

The National Park Service (NPS) began near annual glacier surveys in Yosemite National Park, beginning in 1931 (Harwell, 1931). NPS rangers measured changes in glacier terminus distance from established markers, conducted repeat photography surveys, and cross-sectional profiles of surface height at several glaciers until 1960, and intermittently to 1975 (White, 1976). Surveys conducted after 1941 focused solely on cross-sectional profiles of surface height of Lyell Glacier and repeat photography at Lyell, Maclure, Dana, and Conness glaciers. These reports documented changes in glaciers and provide useful comparisons to present day conditions. Much of the earlier results were compiled into reports by Matthes (1939; 1940).

Sierra Nevada glaciers retreated throughout the 1930s (Matthes, 1940). In the 1940s several reports indicate increases in thickness in the upper portions of glaciers based on repeat photographs of Lyell Glacier (Harrison, 1956) and mapping at Palisade Glacier (Heald, 1947). However, no increase in area was observed. Glacier retreat resumed through out the 1950s and early 1960s (Hubbard, 1954; YOSE, 1960).

During the late-1960s mass balance data was collected at Maclure Glacier for three years beginning in 1966 as part of the 1967 International Hydrologic Year (Tangborn et al., 1977). This study is the only published mass balance work on Sierra Nevada glaciers, and provides insight on accumulation and ablations rates during above average snow years. Yosemite NPS reports of 1970 and 1975 show slight decreases in area compared to the early 1960s (White, 1976). Following the mid 1970s, the available observational record becomes scarce. A repeat photograph survey conducted in 1986 of Lyell, Maclure, Dana, and Conness glaciers by Douglas Hardy found the glaciers in a similar condition as 1975, with an increase in seasonal cover (Yosemite National Park archive). Chambers (1992) conducted studies on Conness Glacier and reported a loss of 5% area in the summer 1991.

The only comprehensive inventory of Sierra Nevada glaciers was conducted by Raub et al. (2006). The survey was based on 1972 aerial photography and compiled a total of 497 glaciers with surface areas ranging between 0.01 and 1.58 km^2. An additional 788 'ice patches' were counted, which "did not meet the definition of a glacier". Topographic variables such as aspect and elevation were recorded for all ice features. This report was completed in 1980 but remained unpublished until 2006.

3. GLACIER POPULATION INVENTORY

Introduction

Glacier inventories summarize the distribution and area extent of glaciers for a region. They are useful for assessing water resources and provide a record of a region's glacier population serving as a valuable baseline to compare with future glacier extents. A comprehensive glacier inventory of the Western US was recently complied by Fountain et al. (2007). As part of this inventory, I conducted an inventory of glaciers in the Sierra Nevada to define the glacier population and extent. The glacier data was compiled in a geographic information system (GIS) database using the methods summarized by Fountain et al. (2007). Glacier outlines are represented as vector polygons. Each polygon is associated with attribute information including location, area, and topographic characteristics.

Methods

The glacier inventory is based on USGS 7.5 minute (1:24,000 scale) topographic quadrangle maps produced from aerial photographs taken between 1975 and 1984. Glaciers are depicted on the maps as white patches with blue contour lines and a blue perimeter and do not distinguish between 'true' glaciers and perennial snow and ice features. Following Fountain et al. (2007), I assume that the glaciers depicted on the topographic maps are perennial snow and ice features, a subset of which are 'true' glaciers.

I downloaded digital versions of all USGS maps that contained glaciers in California from the California Spatial Information Library (http://gis.ca.gov). The digital maps, known as Digital Raster Graphics (DRG), were compiled into a GIS database using ESRI ArcView 9 software (Fountain et al., 2007). I acquired hydrographic line data in Cartographic Feature File (CFF) format (vector) from the US Forest Service (USFS). The USFS digitized all hydrographic lines on USGS topographic maps (e.g., rivers, lakes, glaciers) and assigned a numerical code to each digitized line. I converted the CFF line files to shapefile polygons (ESRI format) and imported the features into the GIS database and extracted only the glacier polygons using the numerical code. The converted glacier polygons were overlaid onto the DRGs to correct errors of shape, omission, and misidentification. Missing glaciers were digitized from the DRGs.

Each glacier polygon was assigned its 'official' USGS glacier name if available, USGS quadrangle name, location (latitude and longitude of centroid), area, topographic characteristics, and quadrangle photographic year acquired from the map collar. The area of each glacier was calculated in the GIS. The topographic characteristics were calculated from 30m Digital Elevation Models (DEM), which I downloaded from the USGS Earth Resources Observation and Science (EROS) Data Center (http://edc.usgs.gov). I summarized the topography (elevation, slope, aspect) of each glacier using zonal statistics; a method that summarizes one type of data (topography) data based on another data type's boundaries (glacier). Uncertainty in the mapped glacier lines on the USGS topographic maps is 12.2m (USGS, 1999; Fountain et al., 2007). I applied a 6.1m buffer to the inside and outside of the glaciers and calculated the total area covered by the buffer. This measure provides an absolute range of uncertainty.

Results

My inventory process identified numerous errors in the CFF data relative to the DRGs. These errors included 53 glaciers missing, which had to be digitized from the DRGs. Over 200 hydrographic features (e.g., lakes) were mistakenly coded as glaciers in the CFF data and were removed. Nine CFF polygons showed uniform glacier cover but the DRG showed rock 'islands' within the glacier boundary and these non-glacial areas had to be removed. Ten extremely small sliver polygons, which were probably artifacts from the original digitization process, had to be removed; Lastly, I split four ice masses into separate glaciers including Palisade, Conness, and Darwin glaciers, and one unnamed glacier below Thompson Peak.

Glaciers were identified on 49 USGS topographic maps (Appendix A) along the Sierra crest from 38.3611 to 36.3861° N and bounded longitudinally between -119.7500° and -118.2561° W. Thirteen glaciers are named, which refer to 34 individual glaciers. For example, the "Matthes Glaciers" refers to a group of 15 glaciers. A total of 1719 glaciers were inventoried ranging in size from 0.0007 ± 0.0007 to 0.8352 ± 0.0329 km^2, a mean of 0.02 km^2, and total area of 39.15 ±7.52 km^2 (Figure 5). The glacier population is dominated by small glaciers with areas <0.05 km^2 (Figure 6). A table with each glacier's record and attribute information is found on the supplemental CD.

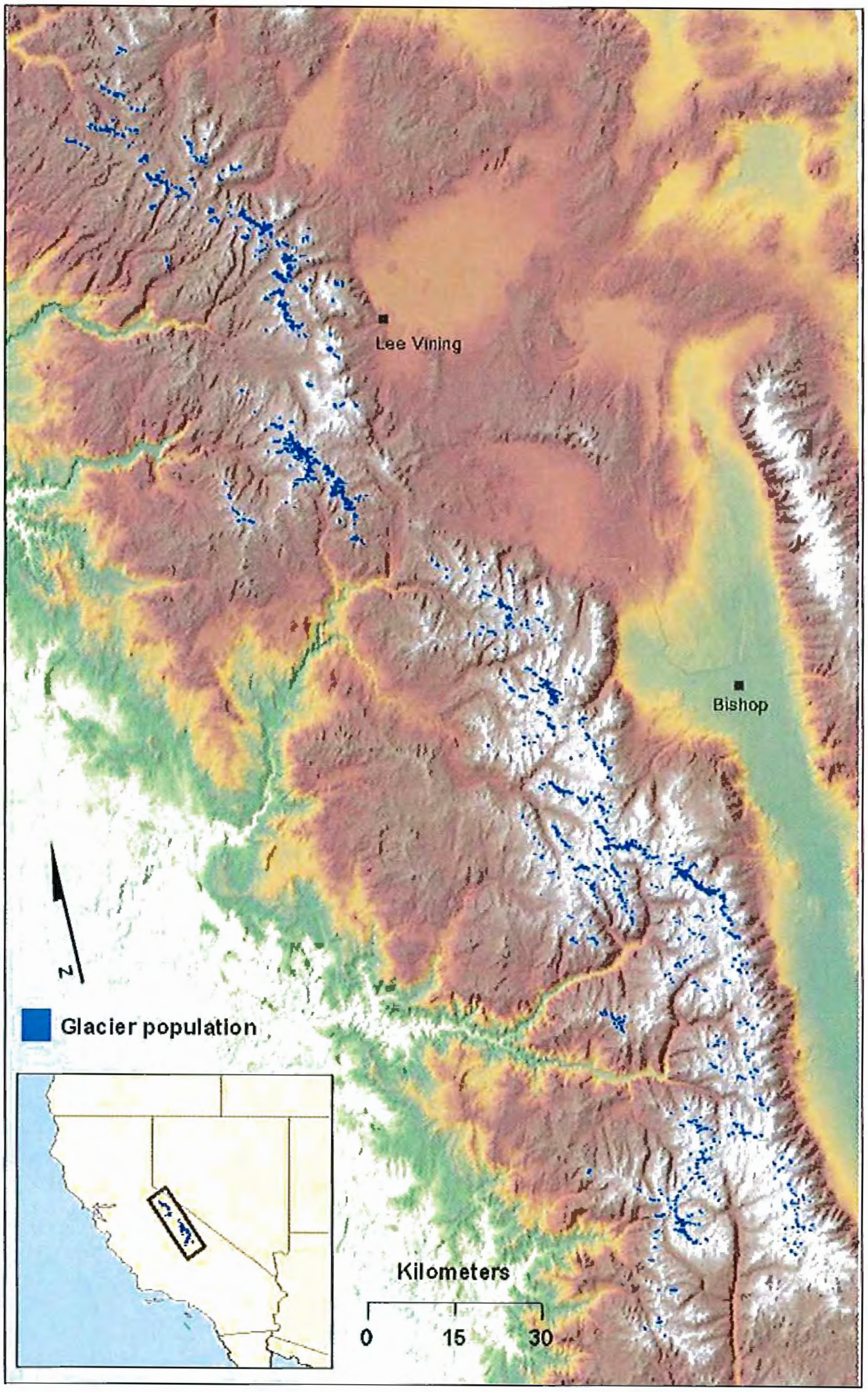

Figure 5. Map of inventory results with glacier population shown in blue.

Glaciers were commonly located on moderate slopes averaging 28° with mean glacier elevations of 2739m to 4263m, and a population mean of 3491m (Figure 6). The mean resultant vector for the population was north-northeast 19° with most having a north to northeast (63%) aspect. Less than 100 glaciers (4%) had southerly aspects. Larger glaciers occupy a smaller range of topographic conditions than the population as a whole, namely higher elevations, moderate slopes, and northern aspects (Figure 7). Smaller glaciers occupy a wider range of topographic conditions.

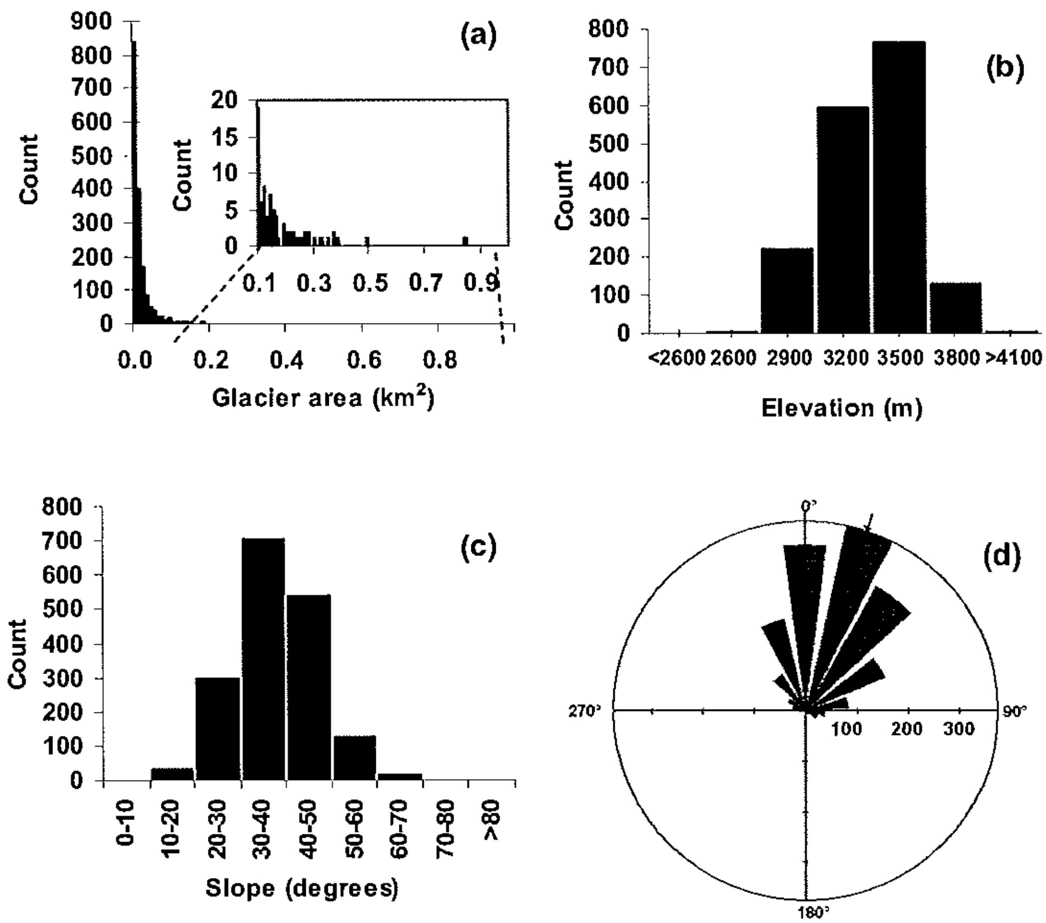

Figure 6. Frequency distribution of (a) glacier area, (b) mean elevation, (c) mean slope, (d) and aspect of the glacier population. Small arrow on aspect plot indicates the population mean resultant vector of 19°.

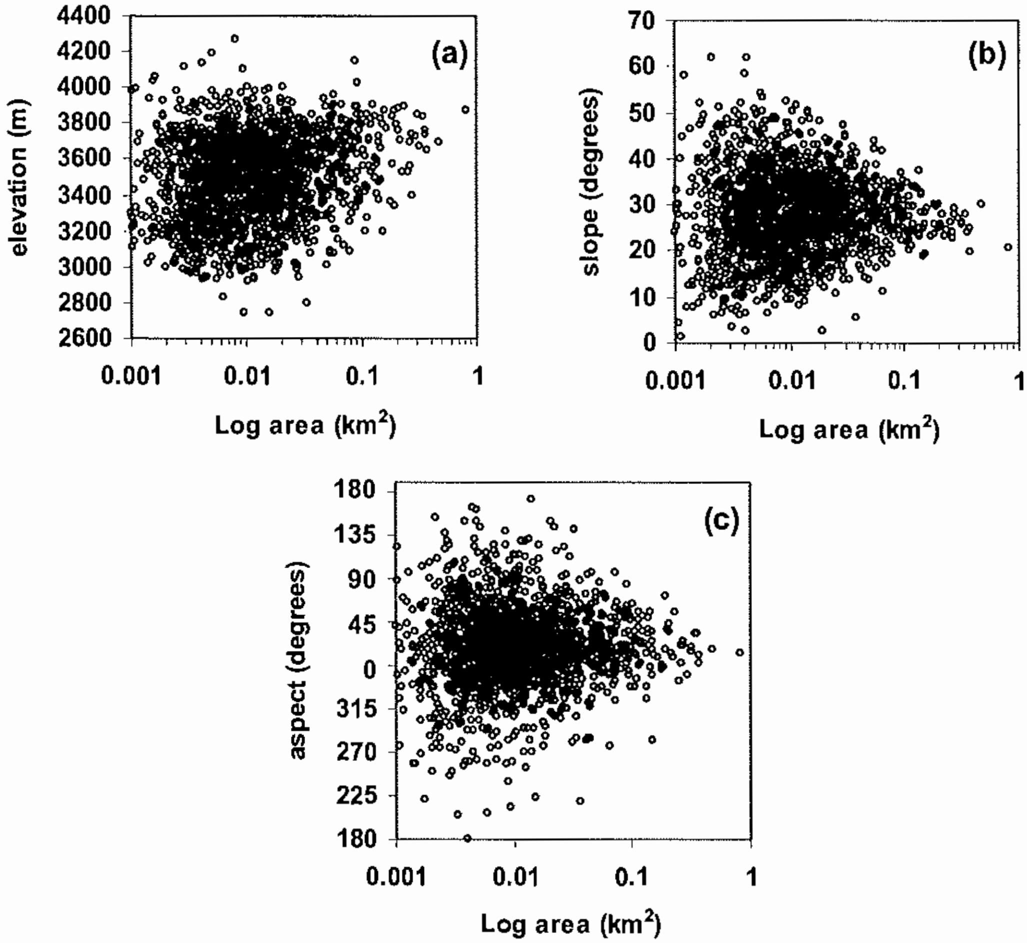

Figure 7. Glacier area plotted with the topographic variables of (a) elevation, (b) slope, and (c) aspect for the glacier population.

I applied two criteria to evaluate ‘true’ glaciers from perennial snow and ice. The first criteria is based on an area threshold of 0.01 km^2, where features <0.01 km^2 are considered perennial snow and ice. This approach follows Raub et al. (2006) and allows my inventory to be directly compared to their findings. The number of “glaciers” under this classification decreases from 1719 to 881, or 51% of my original inventory, and the total area decreases from 39.15 ± 7.52 km^2 to 34.76 ± 5.74 km^2, with a mean glacier size of 0.04 km^2 (Figure 8, Table 1).

The size criterion is an arbitrary classification based largely on the assumption that a real glacier or important glacier requires a certain size. A more objective criterion is the critical shear stress for ice, 10^5 Pa (Paterson, 1999), the theoretical threshold for deformation if ice is assumed to be a perfect plastic. If the shear stress at the bottom of a glacier >10^5 Pa then the glacier deforms (moves). The basal shear stress is given by,

$$\tau_b = \rho_i g h \sin\alpha \qquad (1)$$

where, ρ_i, is ice density (900 kg m^{-3}), g, is gravitational acceleration (9.81 ms^{-2}), h, is ice thickness (m), and, α, is the ice surface slope. The surface slope was derived from the GIS and the DEM. I used the maximum slope of all grid cells within the glacier boundary as a conservative estimate. Average thickness of each glacier was determined from the glacier volume divided by its area. Area is derived directly from the GIS database and volume was estimated from a scaling relation between glacier area and volume (Chen and Ohmura, 1990),

$$V = \alpha A^{\beta} \qquad (2)$$

where, V, is glacier volume (km^3), α, is an empirical constant (0.0358), A, is the glacier area (km^2), and, β, is also an empirical constant (1.3312).

A total of 118 glaciers, or 7% of the glacier population, exceed the critical shear stress of 10^5 Pa with a total area of 15.87 ± 1.69 km^2 (Figure 8). Glacier area ranged from 0.05 to 0.83 km^2 with a mean size is 0.13 km^2. Glaciers with areas >0.15 km^2 all exceed this threshold.

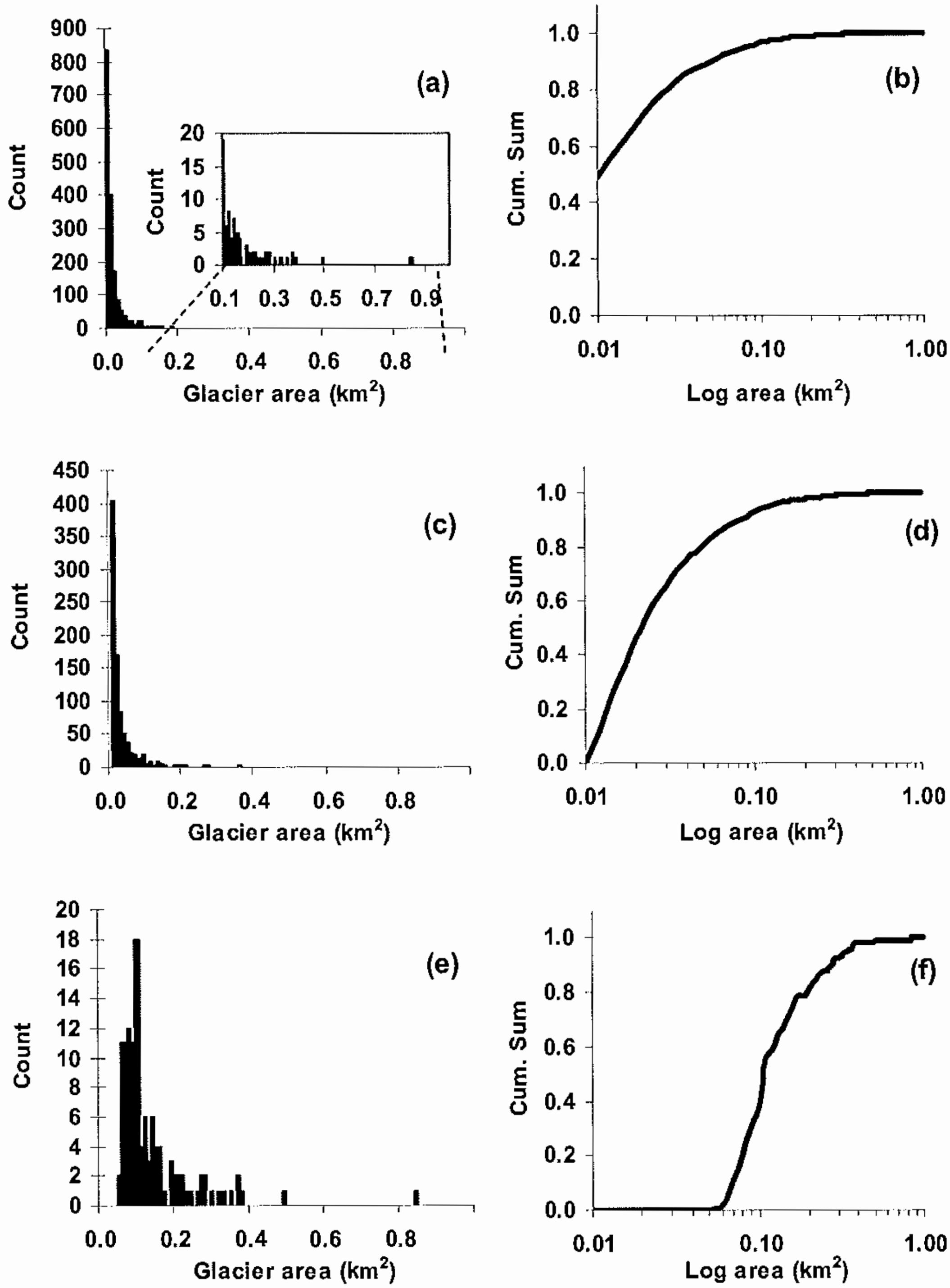

Figure 8. Glacier count (left) and cumulative sum (right) area for all glaciers (a, b), glaciers >0.01km^2 (c, d), and glaciers with basal shear stress >10^5 Pa (e, f). The insert in (a) displays the count of glaciers with area >0.1 km^2. Note change in scale for count in a, c, and e.

Table 1. Comparison of glacier area (km^2) statistics for the glacier population, glaciers with area >0.01 km^2, and glaciers with calculated shear stress >10^5 Pa.

Statistic	Total population	Area >0.01km^2	Shear stress >10^5 Pa
count	1719	881	118
mean	0.0228	0.0395	0.1345
median	0.0103	0.0218	0.0956
minimum	0.0007	0.0100	0.0462
maximum	0.8352	0.8352	0.8352
total	39.1522	34.7647	15.8726

Comparison with previous inventories

Results from glacier inventories rely heavily upon the researcher's definition of a glacier and the area of examination. The published population of glaciers in the Sierra Nevada has been increasing with time because of changing definitions and improved data collection. Kehrlein (1948) identified 49 glaciers and 12 "dying remnants"; all showed movement. Meier (1961) reported 70 glaciers; 69 glaciers with areas < 0.05 km^2 and one glacier with area between 1 and 2 km^2. The Raub et al. (2006) inventory was completed in the late 1970s. They defined a glacier as having a minimum area of 0.01 km^2 and *"any perennial ice exhibiting one or more of the following: (1) snow or ice accumulated over several years, (2) a crevasse, (3) heavily debris-covered ice which exhibits evidence of flow, and (4) moraines or trim lines"* . This inventory included a category for 'ice patches' that did not fit the glacier definition and included snowdrifts, snow accumulation, snowfields, ice pockets, and snow patches >0.005 km^2. Raub et al. (2006) used aerial photography taken in 1972 and modified glacier outlines depicted on 1:62,500 scale topographic maps, producing generalized outlines, not detailed glacier boundaries. They counted 497 glaciers (24.1 km^2) and 788 ice patches (19.1 km^2) for a total count of 1285 (35.1 km^2).

My inventory counted more glaciers with a larger glacier covered area compared to the Raub et al. (2006) inventory (Table 2). However, if I removed glaciers <0.005 km^2, that Raub et al. (2006) did not count, my estimate decreases to 1313 (28 more than Raub et al.) with a total area of 37.9 $km^2 \pm 6.9$ km^2 or 2.7 km^2 greater than Raub et al. (2006). I combined Raub et al.'s glaciers and ice patches that had areas >0.01 km^2 to compare to my inventory and found similar ice covered areas but 174 fewer glaciers than Raub et al. inventory. A comparison of 'true' glaciers between inventories showed that the shear stress criteria resulted in 379 fewer glaciers than Raub et al. and almost half the area. Matching Raub et al.'s count required a shear stress threshold reduction of 40%, resulting in a total area of 28.4 km^2, 4.3 km^2 greater than Raub et al.'s (2006). Matching Raub et al.'s glacier area required a shear stress threshold reduction of 30% that increases my glacier count by 187.

Table 2. Comparison of glacier inventories.

Study	Photograph date	Scale	Count	Total area (km2)	Count (>0.01km^2)	Area (>0.01km^2)
Raub et al.	1972	1:62,500				
All glaciers			1285	35.1	1055	34.9
'true' glaciers			497	24.1	497	24.1
My inventory	1975-1984	1:24,000				
All glaciers			1719	39.15 ± 7.52	881	34.76 ± 5.74
<0.005 km^2 filtered			1313	37.86 ± 6.87	881	34.76 ± 5.74
'true' glaciers (shear stress)			118	15.87 ± 1.69	118	15.87 ± 1.69

The two inventories are similar when Raub et al.'s (2006) minimum size threshold (0.005 km^2) is applied to my inventory yielding a difference of 28 glaciers and an area difference of <3km^2 (8%). The similarities of these values are high considering the different map scales, photography dates, and approaches. Differences between the two inventories increase when comparing glaciers >0.01 km^2, and 'true' glaciers. The >0.01 km^2 comparison showed my inventory counted 174 less glaciers than Raub et al., but total areas were similar. The difference in glacier count is probably from the difference in map scale used. The scale affects the accuracy of area measurements which is important to a large number of glaciers are in this size class (Figure 8b) and therefore sensitive to thresholds of this size. For example, my inventory contains 120 glaciers between the sizes of 0.0090 and 0.0109 km^2. The sensitive size difference is also confounded by the difference in photographic dates of the two inventories, as a small decrease in glacier area between the two inventories would lower the count.

The differences in the 'true' glacier comparison are greater in both count and area because of different glacier definitions. Raub et al. (2006) used visual evidence and may be mistaken in their detection of crevasses or evidence of flow. Furthermore moraines and trim lines are evidence of past movement and not necessarily current activity. My use of numerical estimates of volume and shear stress may be imprecise. Uncertainty exists in the volume-area scaling and the use of a glacier average depth underestimates local depth. My use of maximum slope for each glacier may compensate, but to what degree is unknown. Consequently, I consider the two inventories of 'true' glaciers to be entirely different.

Granshaw and Fountain (2006) used nearly identical methods to mine to compared their digital inventory of glaciers in the North Cascades, Washington, with an inventory by Post et al. (1971), which used nearly identical methods as Raub et al. (2006). Granshaw and Fountain counted more glaciers (+575) and had a greater total area (+12.5 km^2) than Post et al. (1971) because of different glacier definitions. Post et al. (1971) had eliminated isolated snow patches used a minimum glacier area of 0.01 km^2 as part of their definition. Results improved when Granshaw and Fountain (2006) filtered glaciers <0.1km^2 from their inventory and removed 93 glaciers from the Post et al. (1971) inventory, which they recalculated to be <0.01 km^2. The filtered results reduced the Granshaw and Fountain (2006) total from 896 to 198 glaciers and the Post et al. (1971) total from 321 to 228 glaciers, a difference of 30 glaciers. Granshaw and Fountain (2006) also filtered their results to match the 321 glaciers inventoried by Post et al. (1971), and found their inventory estimated 1.7 km^2 more glacier area than Post et al. (1971). Given the differences in map scales used and differing methods, the inventories were similar. The digital map inventories by Granshaw and Fountain (2006) and my inventory in the Sierra Nevada both resulted in higher numbers of glaciers and greater total areas. Filtering the results to match definitions of the inventories of Post et al. (1971) and Raub et al. (2006) show the inventories digital and hand drawn inventories are similar.

4. GLACIER CHARACTERISTICS AND TEMPORAL CHANGE

In this chapter I reconstruct past and present extents for a subset of 14 glaciers using geologic evidence, photographs, and field measurements. I combine these data into a GIS database of glacier extents and quantified the magnitude of change for 14 glaciers and estimate the rate of change at seven glaciers.

Study Glaciers

I selected a subset of glaciers for study based on location, minimal debris cover, and availability of historical data. I wanted to have a minimum of two sites in each of the three national parks in the Sierra Nevada (Yosemite, Kings Canyon, and Sequoia) because the NPS is interested in understanding changes in high alpine ecosystems and provided funding for fieldwork to assess glacier change (Mutch et al., 2006). The three parks have a north-south orientation providing the latitudinal range needed to assess differences in solar radiation, temperature, and precipitation. Selected glaciers have a minimum surface cover of rock debris because it obscures the glacier margins and the insulating properties of debris alters the glacial response to climate change (Konrad and Humphrey, 2000). These criteria eliminated relatively large Palisade Glacier. Based on these criteria, 14 glaciers were selected (Table 3 and Figure 9) with a subset of seven glaciers selected to infer temporal changes during the past century. Many of the selected glaciers are unnamed on the USGS topographic maps. I applied informal names based on nearby mountains for Dragontooth, Dana, West Lyell, East Lyell, Goddard, Middle Goddard, Black Giant, Brewer and Picket glaciers.

Table 3. Locations of the study glaciers. Names in bold are those selected for in depth study over time. Names in italics are informal glacier names. Area and topographic characteristics are based on the population inventory. Elv = elevation (meters), Slp = slope (°), Asp = aspect (°).

Glacier	Latitude	Longitude	Area(km^2)	Elv	Slp	Asp
Dragontooth	38.1009	-119.3861	0.1819	3359	24	0
Conness	37.9695	-119.3192	0.2641	3561	23	20
Dana	37.9020	-119.2195	0.1372	3598	37	37
Maclure	37.7467	-119.2827	0.2631	3689	24	2
West Lyell	37.7430	-119.2722	0.3686	3762	20	1
East Lyell	37.7439	-119.264	0.3733	3648	25	11
Darwin	37.1712	-118.6768	0.1572	3871	29	9
Middle Goddard	37.1096	-118.7137	0.0718	3697	32	4
Goddard	37.1075	-118.703	0.2965	3732	27	349
Black Giant	37.1056	-118.6474	0.0915	3630	34	52
Middle Palisade	37.0753	-118.4686	0.2002	3787	30	37
Brewer	36.7104	-118.4821	0.0833	3808	30	21
Lilliput	36.5723	-118.5532	0.0481	3361	31	336
Picket	36.5593	-118.5082	0.3655	3734	24	33

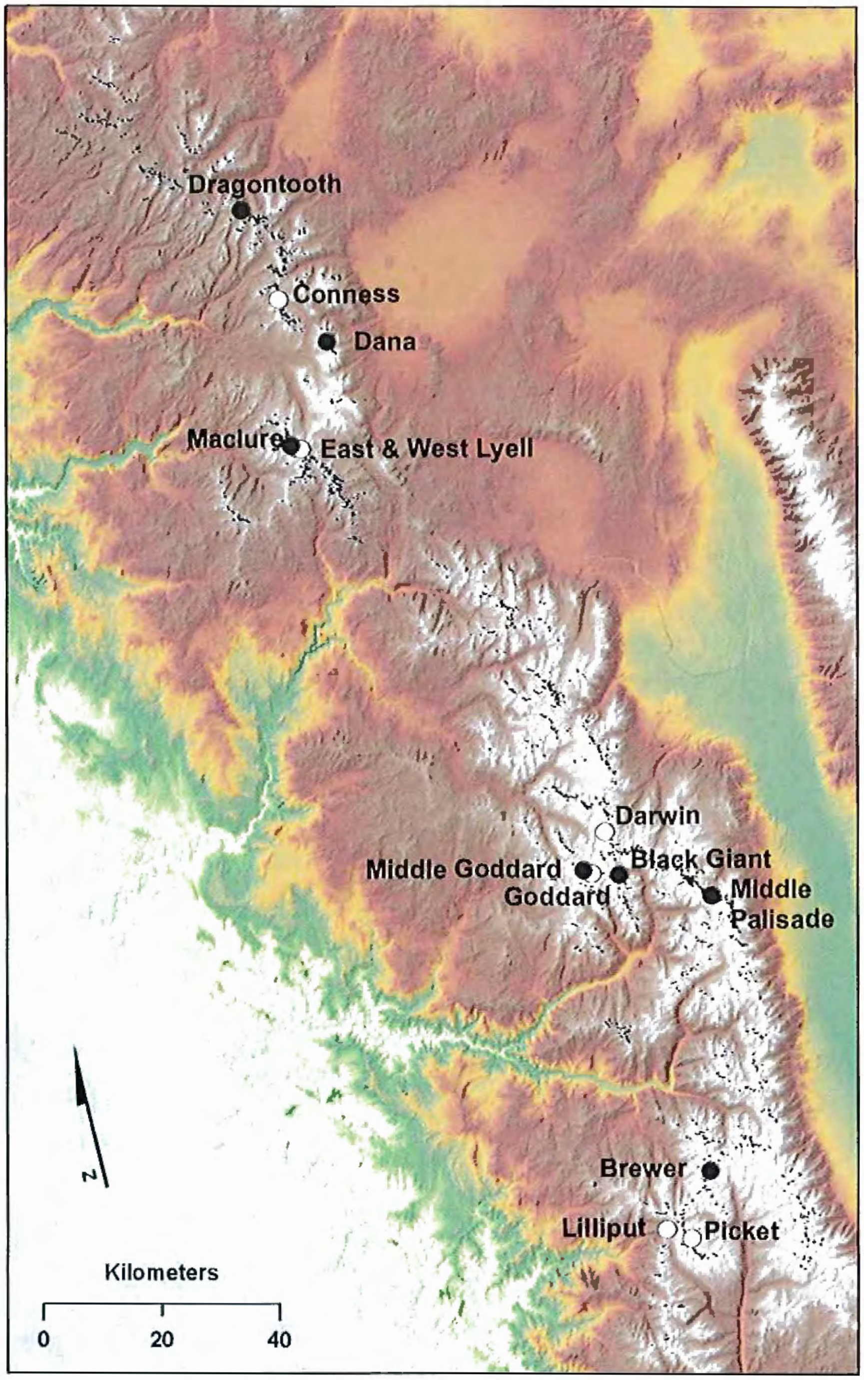

Figure 9. Location of the 14 glacier study sites. Solid circles indicate study sites where total change was calculated. White circles indicate glaciers for in depth study of change. East and West Lyell are considered separate study sites. Glacier population appears in dark grey.

Dragontooth Glacier is located on the north side of Sawtooth Ridge, in the Toiyabe National Forest, north of Yosemite National Park (Figure 10a). The glacier is located on the north side of an unnamed peak referred to as 'The Dragontooth' (3681m). This glacier is at the headwaters of Robinson Creek, a tributary of the Walker River.

Dana Glacier is at the head of Glacier Canyon, located in the Inyo National Forest, and contributes to Lee Vining Creek (Figure 10b). Dana Glacier is on the northeast side of Mount Dana (3981m).

Conness Glacier is located in the Inyo National Forest, just east of Yosemite National Park and the Sierra crest at the headwaters of Lee Vining Creek, which flows into Mono Lake (Figure 10c). The glacier is located below Mount Conness (3838m) and has two lobes. Only the western main lobe is used in this analysis because the eastern lobe remains snow covered making it difficult to determine the boundary.

Lyell and Maclure glaciers are located at the headwaters of the Tuolumne River in eastern Yosemite National Park (Figure 10d). The Lyell Glacier consists of two distinct lobes separated by a rock ridge. I separate the east and west lobes into separate study sites because they occupy separate cirques and flow independently. West Lyell Glacier is located below Mount Lyell (3998m) and East Lyell Glacier is below an unnamed peak (3927m). Maclure Glacier is located just north of the Lyell Glaciers on the north side Mount Maclure (3951m).

Darwin, Goddard, Middle Goddard, and Black Giant glaciers are located in northern Kings Canyon National Park. Darwin Glacier is located on the north side of

Mount Darwin (4216m) at the headwaters of a tributary to Evolution Creek that flows to the San Joaquin River (Figure 10e). Black Giant Glacier is located on the north side of Black Giant (4063m) at the headwaters of the Middle Fork Kings River (Figure 10f). Goddard Glacier is located on the northeast side of Mount Goddard (Figure 10g). Middle Goddard is located just west of Goddard Glacier in an adjacent cirque. Both glaciers are at the headwaters of North Goddard Creek, a tributary of the San Joaquin River.

Middle Palisade Glacier is located on the north side of Middle Palisade (4271m) east of the Sierra Crest in Inyo National Forest at the headwaters of the South Fork of Big Pine Creek (Figure 10h). Middle Palisade Glacier is composed of two cirque glaciers. I selected the more northerly feature because surface was free of rock debris.

Brewer, Lilliput, and Picket glaciers are located along a mountain sub-range known as the Great Western Divide. Brewer Glacier is located on the northeast side of Mount Brewer (4136m) at the headwaters of a tributary to East Creek in southern Kings Canyon National Park (Figure 10i). Lilliput and Picket glaciers are located in Sequoia National Park. Lilliput Glacier is located on north side of Mount Stewart (3721m) at the headwaters of Lone Pine Creek, a tributary of the Middle Fork Kaweah River (Figure 10j). Picket Glacier is situated between Mount Lawson (4000m) and Queen Kaweah (4080m) at the headwaters of Picket Creek, a tributary of the Kern River (Figure 10k).

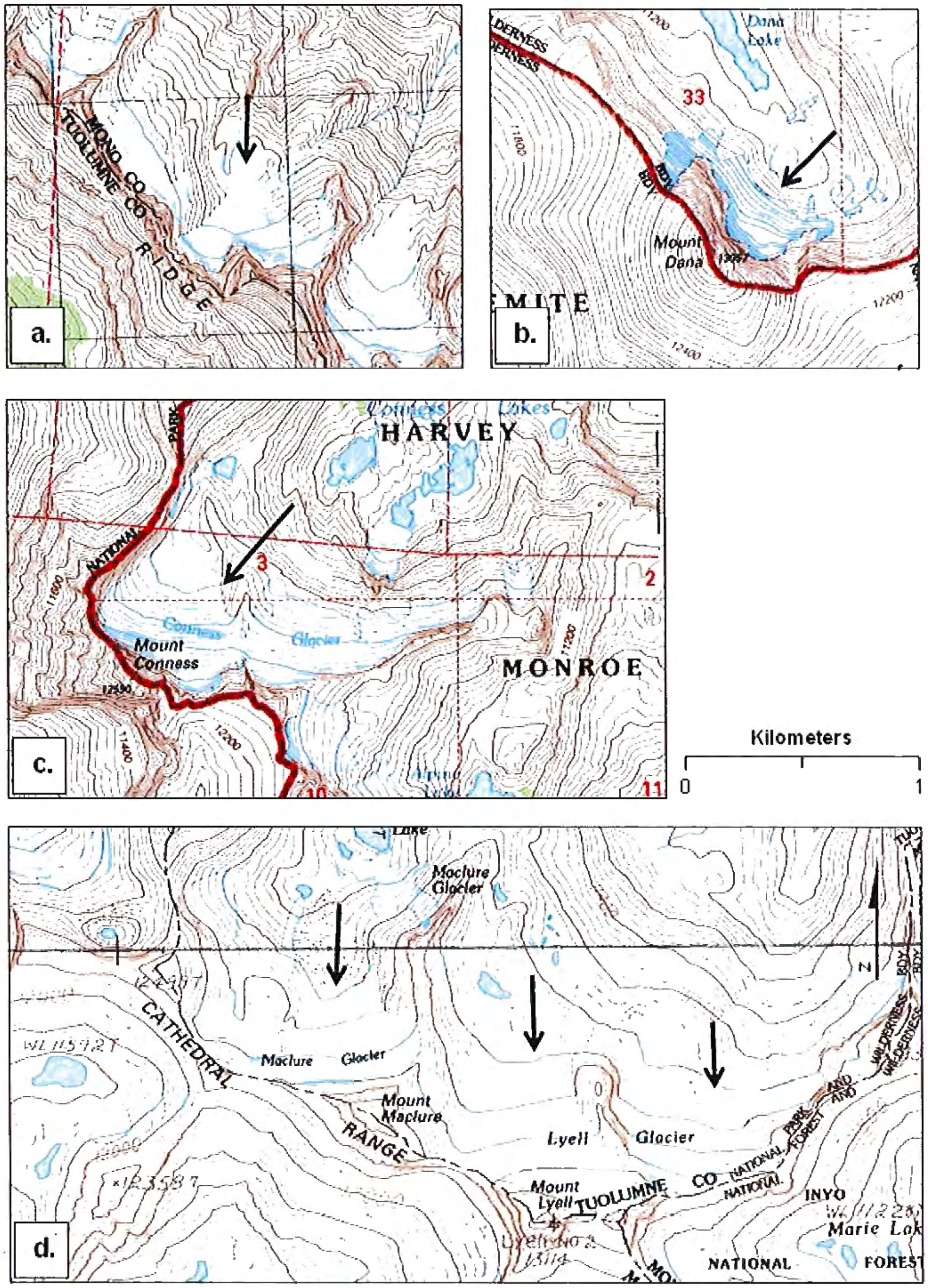

Figure 10. Study site glaciers identified on topographic maps (1:24,000) including (a) Dragontooth Glacier, (b) Dana Glacier, (c) Conness Glacier, and (d) Maclure, West and East Lyell glaciers. Maps are copies of USGS quads: Matterhorn Peak (1984, 1985) for (a), Tioga Pass (1984) for (b) and (c), and Mount Lyell (1984) for (d).

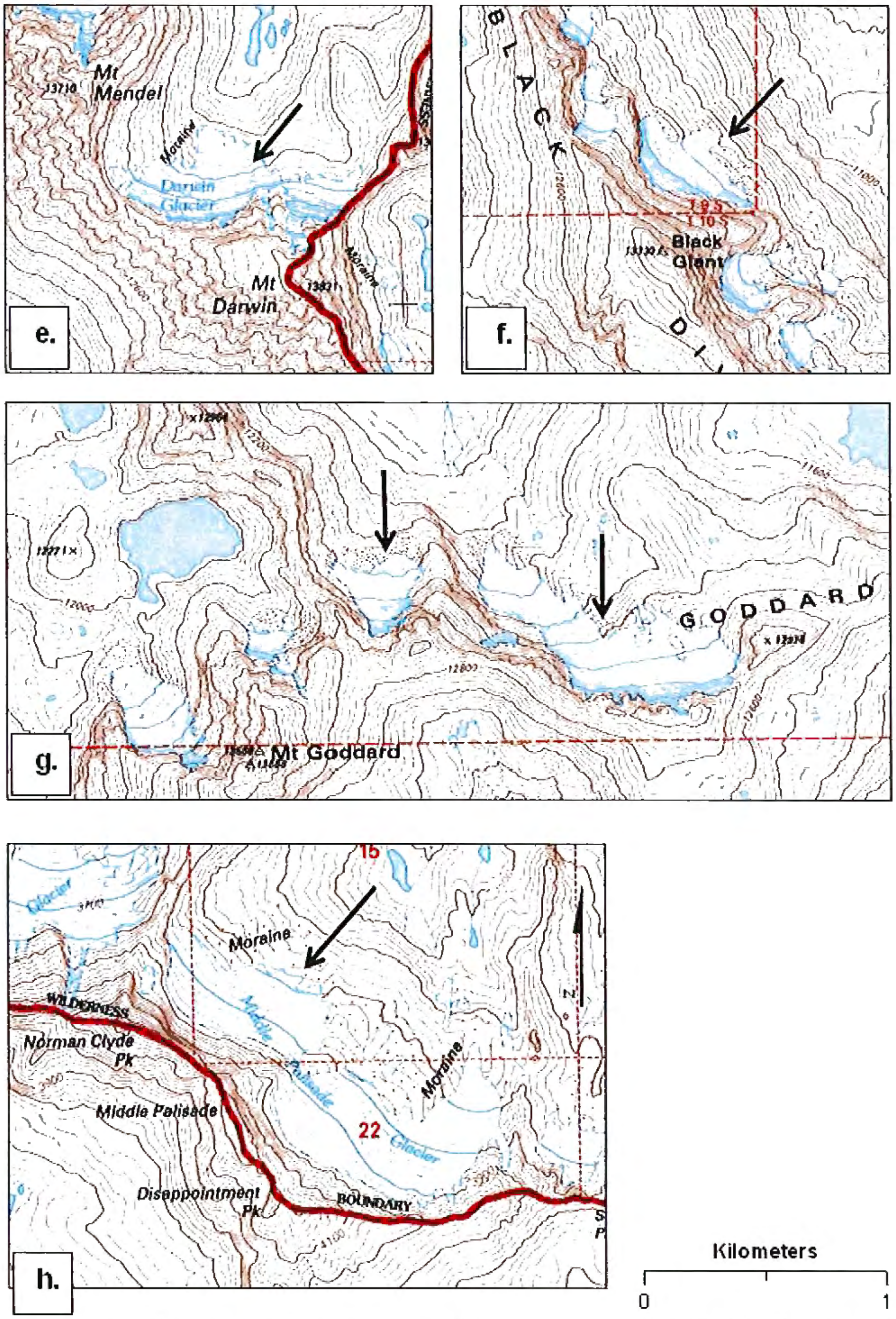

Figure 10 continued. Study site glaciers (e) Darwin Glacier, (f) Black Giant Glacier, (g) Middle Goddard (left) and Goddard (right) and (h) Middle Palisade Glacier. Maps are copies of USGS quads: Mount Darwin (1976) for (e), Mount Goddard (1976) for (f) and (g), and Split Mountain (1975) for (h).

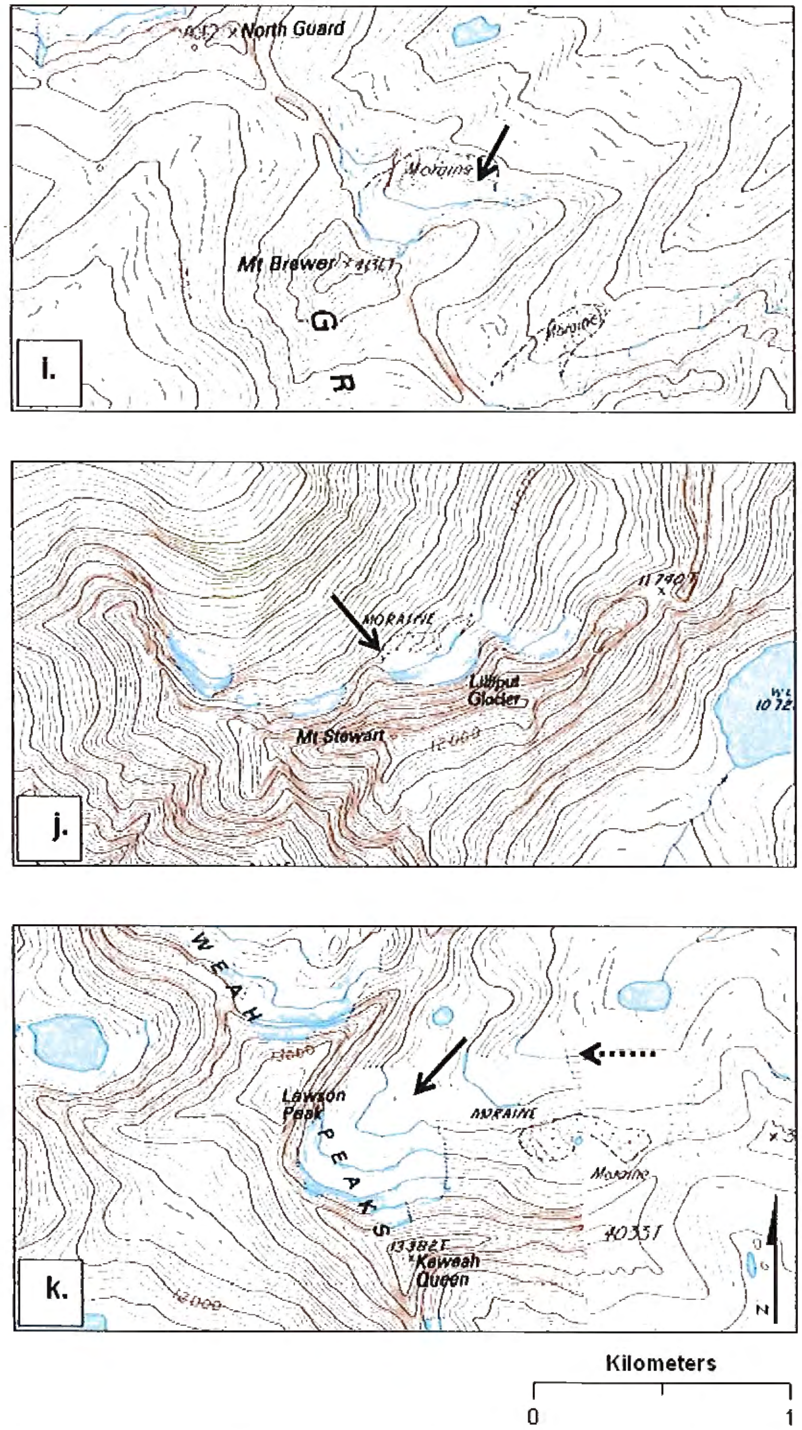

Figure 10 continued. Study site glaciers (i) Brewer Glacier, (j) Lilliput Glacier, and (k) Picket Glacier. Maps are copies of USGS quads: Mount Brewer (1976, 1978) for (i), and Triple Divide Peak (1976, 1978) for (j) and (k).

The 14 study glaciers and their distribution are representative of the glacier population in the Sierra Nevada (Figure 9). Four study glaciers are <0.10 km2 (Table 4 and Figure 11), which account for 96% of the glacier population >0.01 km^2. The remaining 10 study glaciers are larger than most in the Sierra Nevada and are distributed among the other area size classes up to 0.40 km^2. Glaciers <0.05 km^2 are not represented. However, glaciers <0.05 km^2 do not meet the shear stress criteria for movement (10^5 Pa) and are therefore not likely to be 'true' glaciers. All 14 study glaciers exceed the shear stress criteria, except for Lilliput Glacier (0.8 x 10^5 Pa).

Table 4. Size comparison of glaciers >0.01 km^2 and selected study glaciers.

Area (km^2)	Count	Cumulative %	Study glacier (count) and name
0.01 - 0.10	821	93.2	(4) Lilliput, Middle Goddard, Brewer, Black Giant
0.11 - 0.20	40	97.7	(4) Dana, Darwin, Dragontooth, Middle Palisade
0.21 - 0.30	12	99.1	(3) Maclure, Conness, Goddard
0.31 - 0.40	6	99.8	(3) Picket, East Lyell, West Lyell
0.41 - 0.50	1	99.9	
0.51 - 0.60	0	99.9	
0.61 - 0.70	0	99.9	
0.71 - 0.80	0	99.9	
0.81 - 0.90	1	100.0	

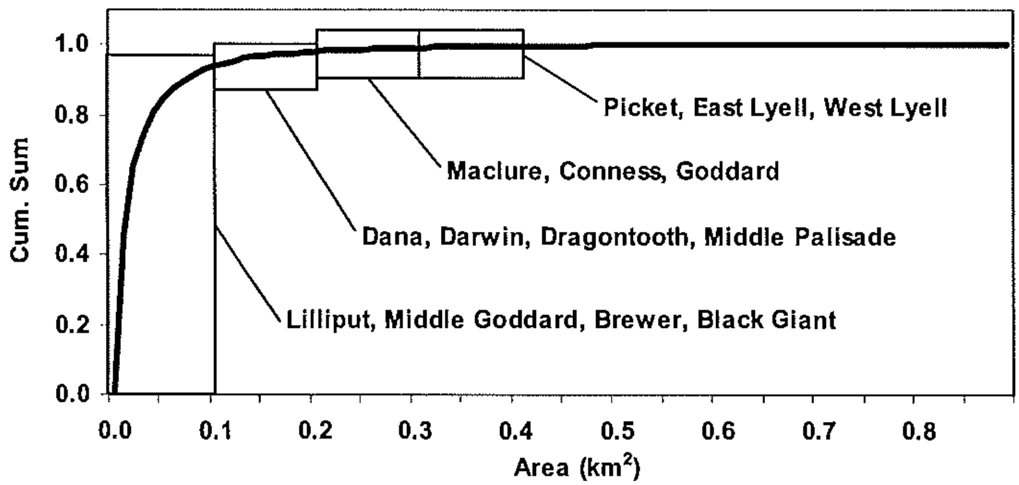

Figure 11. Cumulative sum of glacier population (>0.01km^2) by area and study glaciers.

The topographic characteristics of the study glaciers (Table 3) are similar to the glacier population (Figure 6). Mean elevations of the study glaciers ranged 500 m with a higher mean (3660 m) as compared to the overall glacier population (3491 m) (Figure 12). Lilliput had the lowest mean elevation (3361 m) and Darwin Glacier had the highest (3871 m). There was no difference in slope angle of the study glaciers and the general population (28°). Aspect varied minimally between glaciers, all were between northwestern and eastern orientation. The study glaciers had a mean resultant vector of 10° compared to the population mean of 19°.

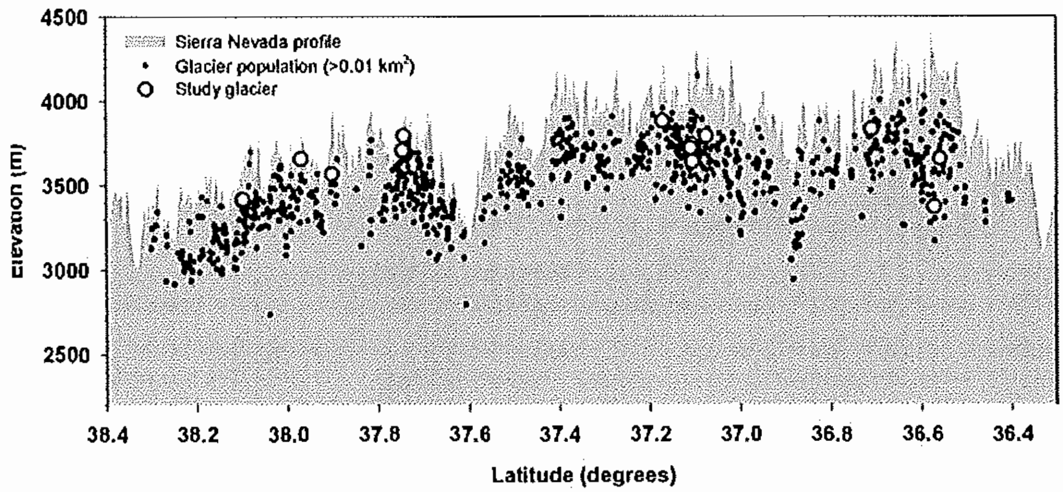

Figure 12. The north to south distribution of the glacier population >0.01 km^2 (black dots) and study glaciers (white circles) plotted with elevation.

Temporal change database

I gathered data on past glacier extents archived at Sequoia and Yosemite National Parks, Inyo USFS Supervisors Office, the USGS Photo Library Archive (USGS, 2006), and the National Agriculture Imagery Program (NAIP). The data included aerial and ground-based photographs, reports, and maps. Yosemite National Park archives included glacier survey reports from 1931 to 1975. Digital maps, aerial photographs and Digital Orthophoto Quadrangles (DOQ) were acquired from the USGS Earth Resources Observation Systems (EROS) Data Center (EDC). The DOQs include encoded positional data and aided in change assessments from unrectified aerial photographs. All data (maps and photographs) are listed in the Appendix. No satellite imagery was used because of the small size of glaciers relative to the spatial resolution of the imagery.

The earliest glacier area data were recorded by I.C. Russell (1885). This report featured photographs of Lyell and Dana glaciers and a map of Lyell Glacier from 1883. In the early 1900s, G.K. Gilbert (USGS, 2006) took photographs of Conness and Lyell glaciers in 1903, Dana Glacier in 1907, and Darwin and Goddard glaciers in 1908. In 1931, Yosemite National Park started to collect nearly annual surveys that included photographs of Lyell, Dana, and Conness glaciers (YOSE, 1931). The first aerial photographs of the glaciers began in 1944, becoming more common in the 1970's.

The maximum extent of the LIA glaciers are preserved by the Matthes moraines (Matthes, 1940; Clark and Gillespie, 1997). Photography at the turn of the last century confirms the ice was in contact with these moraines in 1903 (Gilbert, 1904; Curry, 1969). I used both the photographic evidence and Matthes moraines to estimate the maximum extent by assuming all glaciers were in contact with the moraines in 1900. I digitized the moraine crest from the earliest aerial photograph. I also used ground-based photographs from the Yosemite National Park glacier reports to estimate glacier extents between the LIA maximum and the availability of aerial photographs. I preferred vertical aerial photography because of scale issues with oblique photography. I used ground-based photography at Lyell Glacier because many were available. The timing of all photographs is important to delineating glacier boundaries. Residual winter snows can hide glacier boundaries, making delineation difficult, if not impossible. Therefore, I only used photos taken in late summer when the ice boundary was visible. Color and texture were helpful to differentiate between snow, ice, and rock.

I field mapped the glacier boundaries at Dana, Maclure, and Lyell glaciers in August 2003, and Conness, Dana, Maclure, Lyell, Darwin, Goddard, Middle Goddard, Black Giant, Lilliput, and Picket glaciers in August and September of 2004. I walked the lateral and terminal boundary while collecting positional data with a Garmin Legend Global Position System (GPS) unit in 2003 and a more accurate Trimble Geo3 GPS in 2004. I collected data every 15 seconds with the Garmin in 2003, with accuracy ± 5 m. I collected point data with the Trimble in 2004, averaged over 15 seconds, and post-processed afterward using PathFinder software and two regional base stations located in Portville and Mammoth Lakes, California, for a final accuracy ± 3 m. Where identification of the glacier boundary was difficult to define because of rock debris, I defined the glacier edge as the boundary where ice could no longer be observed. All GPS data was collected in the NAD 27 UTM Zone 11. Additionally, I rephotographed the glaciers and attempted to match the same perspective and camera locations as the historic photographs following repeat photographic methods outlined by Harrison (1960) and Klett et al. (1984).

I constructed a temporal record of areal change by importing the USGS DOQ imagery, digital maps, and the scanned aerial photographs for each glacier into the GIS database using ArcGIS software. All data were projected in North American Datum (NAD) 1927 UTM Zone 11; Clarke 1866 geodetic model. I georeferenced the aerial photographs to the DOQ imagery using boulders and rock features as control points. I reduced the georeferencing error caused by the steep and complex topography surrounding the glacier using 7 to 10 control points close each glacier, especially near the lower glacier boundary where change is typically the greatest. The number of control points used for each glacier depended on glacier size and geometry. The RMSE georeferencing of aerial photographs was maintained between 7 and 12m. Once the imagery was georeferenced, I digitized the glacier perimeter into a polygon, creating separate polygon shapefiles for each temporal depiction.

I imported my 2003 and 2004 GPS data into a GIS and converted the data into polygon shapefiles by connecting GPS points. The upper unmapped portion of the glacier typically changed very little and was interpreted from the USGS DOQs. I calculated the area and perimeter for each polygon shapefile and included attributes of glacier name, date of depiction, and source (aerial or ground-based photograph, GPS field mapping, or geologic evidence). For aerial and ground-based photographs I included the source and date of each photograph. I also included a measure of uncertainty produced from the georeferencing process and GPS error.

I calculated the uncertainty of the glacier depictions by buffering each depiction based on a calculated distance (Granshaw, 2002; Nylen, 2004; Granshaw and Fountain, 2006). The magnitude of uncertainty associated with the glacier depictions is specific to each type of source. For aerial photographs, I based the buffer distance on the georeferencing RMSE, typically ± 8m. The buffer distance used for GPS mapping data is based on the positional accuracy of the data, typically ± 3 to 5 m. The uncertainty of ground-based photographs is more difficult to determine because of inconsistent scale and a lack of suitable landmarks. I estimated the uncertainty based on the distance between glacier depictions, typically 10m, and used this distance as an uncertainty estimate. While somewhat arbitrary, the estimate is conservative when applied to the entire glacier boundary. In all cases, I buffered both the inside and outside of each glacier polygon in order to calculate the range of uncertainty.

Results

Locating aerial photos with low snow cover was a reoccurring problem, particularly in the 1980s and 1990s. The combination of above average snow years and early season aerial photography resulted in many potentially useful photo years to be discarded. Identifying moraines defining the LIA extent was also problematic because of the internal melting of their ice cores which caused deflation. Beatty (1939) noted the presence of ice in Matthes moraines. I observed ice present in the Conness and Goddard glacier moraines in 2004. I estimated the LIA boundary from the earliest aerial photography available in conjunction with field mapping. Rock debris on the glacier surface occasionally made field mapping of the glacier boundary difficult, notably on Conness, West Lyell, and Goddard glaciers.

Photographs taken between 1903 and 1909 confirm the glaciers were near or at their Matthes moraines as shown in the repeat photographs. All glaciers were assigned a 1900 extent based on moraines evidence and early photographs. No early photographs were found at Middle Palisade or Mount Brewer glaciers, so I relied on the moraine evidence to reconstruct the 1900 extent. Recent glacier extents for 2003 to

2006 were based on field GPS data and aerial photos. The number of depictions of each glacier varied depending on data availability (Table 5).

Table 5. Study glaciers with the number of extents and time range of available data. Names in bold are those selected for in depth study over time. Asterisk indicates extent based solely on moraine position.

Glacier	Number of Extents	Time range of source data
Dragontooth	2	1905 - 2006
Conness	5	1901 - 2004
Dana	2	1903 - 2003
Maclure	2	1903 - 2003
West Lyell	8	1903 - 2004
East Lyell	12	1903 - 2004
Darwin	5	1908 - 2004
Middle Goddard	2	1907 - 2004
Goddard	4	1908 - 2004
Black Giant	2	1909 - 2004
Middle Palisade	2	1900*-2005
Brewer	2	1900*-2005
Lilliput	4	1973 - 2004
Picket	3	1973 - 2004

I compared my assessment of area from the 1972 – 1973 photographs against the Raub et al. (2006) inventory and the map-based inventory based on 1976 – 1984 photography described in Chapter 3. As mentioned the Raub et al. (2006) inventory is based on 1972 photography. The results are generally similar (Figure 13). Glacier areas estimated by Raub et al. (2006) were higher in 4 out of 7 cases. The map-based results were higher in 6 of 7 cases. The larger area found by Raub et al. (2006) is related to the method of area calculation. The larger area of the map-based may be caused by the difference in photographic dates, especially Conness, West Lyell, and East Lyell which are based on photography 12 years later. The most extreme difference was at Picket Glacier, where the map-based inventory overestimated glacier area by 250%. This was likely caused by an error caused by including residual winter snow as evident from the pattern and shape of the map depiction of the glacier (Figure 10k).

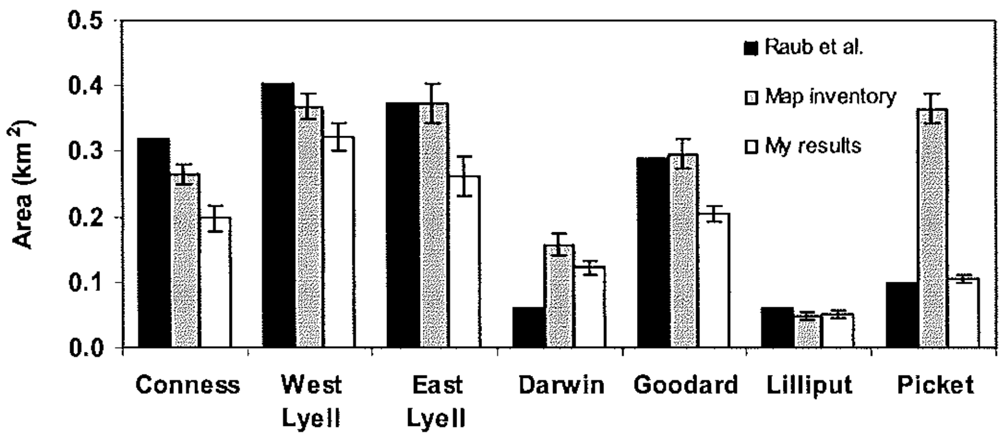

Figure 13. Comparison of glacier area calculated by Raub et al. (2006) inventory based 1972 aerial photographs, the map-based inventory (Fountain et al., 2007) based on aerial photos from 1984 of Conness, West Lyell, and East Lyell glaciers, 1976 of Darwin, Goddard glaciers, and 1975 of Lilliput and Picket glaciers, and the glacier extents I defined (this chapter) based on 1972 - 1973 aerial photography.

I totaled the area of the seven glaciers to compare the three methods (Table 6). The Raub et al. (2006) and map inventories are similar differing by 0.26 km^2. My results were less than the Raub et al. (2006) by 0.34 km^2 and the map inventory by 0.61 km^2. I attribute the difference to the scales used in each method. Raub et al. (2006) mapped glaciers at 1:62,500 versus the map inventory at 1:24,000 and my depiction were finer than 1:10,000. The finer scale allowed my depiction to be more detailed compared to the generalized lines of the Raub et al. (2006) and map inventories. The difference in photograph years may have also caused differences. Photographs for the map inventory, which had a greater total and mean area, were acquired 3 and 12 years after the inventories. A glacier advance or increased snow cover would increase the area.

Table 6. Comparison of three methods for the total area (km^2), standard deviation (std dev) and mean area of the seven glaciers.

	Photo year	Total area (km^2)	Std dev (km^2)	Mean (km^2)
Raub et al.	1972	1.611	0.151	0.230
Map inventory	1975 - 1984	1.8731 ± 0.7703	0.1358	0.2682
My results	1972 - 1973	1.2668 ± 0.0459	0.0945	0.1810

A total of 52 repeat photographs were collected from ten glaciers during the summers of 2003 and 2004 revealing the glaciers have retreated, thinned, and have a deflated or concave appearance. Rock debris appears to have increased over time on Darwin and Goddard glaciers, but this was not quantified. Six photographic pairs have been included in the Appendix for Darwin, Goddard, Lyell, Maclure, Dana, and Conness glaciers.

All 14 glaciers decreased in area over the past century with a total loss of 2.14 km^2 ± 0.10 (56%), ranging from 0.02 km^2 ± 0.01 (31%) at Lilliput Glacier to 0.49 km^2 ± 0.05 (78%) at the East Lyell Glacier, with an average of 0.15 km^2 (Figure 14). On average, the 14 glaciers lost 55% of their area since 1900. Source and error data for each glacier depiction are compiled in the Appendix. The rate of glacier change varied between the seven glaciers (Figure 15). The first recorded change occurred at East Lyell Glacier, which lost 0.07 km^2 (12%) by 1923. Rapid retreat continued through the 1930s and 1940s. The highest rate of loss at East Lyell Glacier occurred between 1931 and 1944, at a rate of $-8360 \text{ m}^2 \text{ y}^{-1}$, a total loss of 0.11 km^2 (Appendix). The highest rate for West Lyell Glacier was recorded between 1944 and 1955, $-6105 \text{ m}^2 \text{ y}^{-1}$, totaling 0.07 km^2. West Lyell and Conness glaciers lost about 25% of their area over the first half of the century and East Lyell and Darwin glaciers lost about 50%. Overall, glaciers continued to retreat between the 1950s and early 1970s, but at a slower rate. Unfortunately, records between the early 1970s and 1990s are scarce or were discarded because of snow cover. Several glaciers advanced during this period, such as East Lyell, Darwin and Lilliput glaciers. The few data since 1970 preclude an assessment of exact timing. In the early 2000s the glaciers continued their retreat. While the rate of change was variable between glaciers there is broad agreement in the temporal pattern of change among the glaciers.

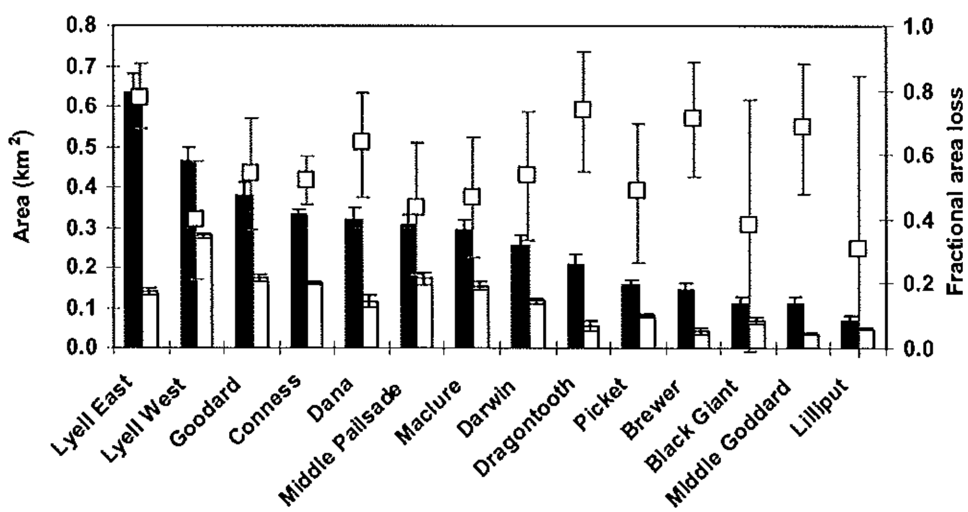

Figure 14. Glacier area in 1900 and 2004 for 14 glaciers in the Sierra Nevada, ordered by original area. Black bars represent glacier area in 1900, open bars represent the 2004 area, and the open squares represent fractional area loss. Uncertainty is represented by error bars.

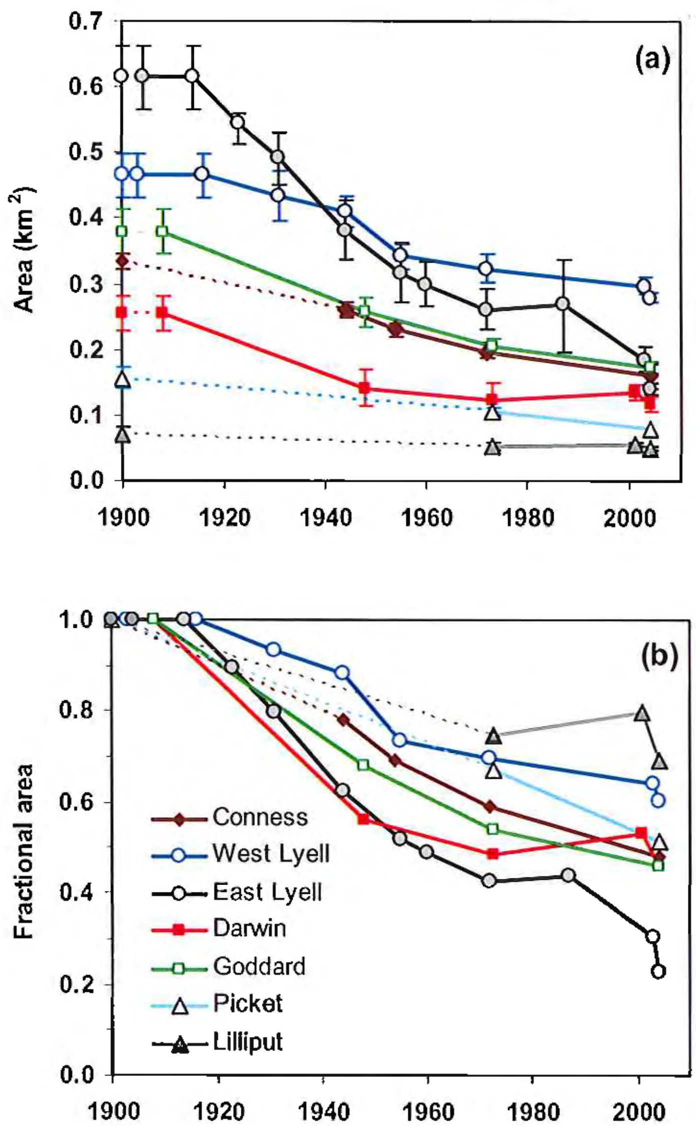

Figure 15. Surface area (a) and fractional area (b) changes at 7 glaciers in the Sierra Nevada over the past century (1900 – 2004). Dashed lines represent assumed change for glaciers lacking early 1900s photographic evidence.

I estimated area change for all glaciers using an area-weighted measure based on the sum of the seven glacier areas. Gaps between measurements were linearly interpolated (Figure 16). The total area lost over the 104-year period was 1.29 ± 0.08

km², or 56% of the original 1900 area of 2.29 ± 0.08 km² (Table 7).These data reveal rapid glacial retreat over the first half of the century, slowed retreat from late 1950s to 1980s, stabilizing 1980s and early 1990s, before returning to a dramatic retreat in the late 1990s (Figure 16).

Table 7. Glacier area totals (km²) in 1900 and 2004 and percent area change for 14 glaciers, and the subset seven glaciers.

	1900 total area (km²)		2004 total area (km²)		Total area loss (km²)		Area change (%)
14 glaciers	3.7862	± 0.0974	1.6426	± 0.0338	2.1435	± 0.1031	- 57
7 glaciers	2.2893	± 0.0774	0.9985	± 0.0166	1.2908	± 0.0791	- 56

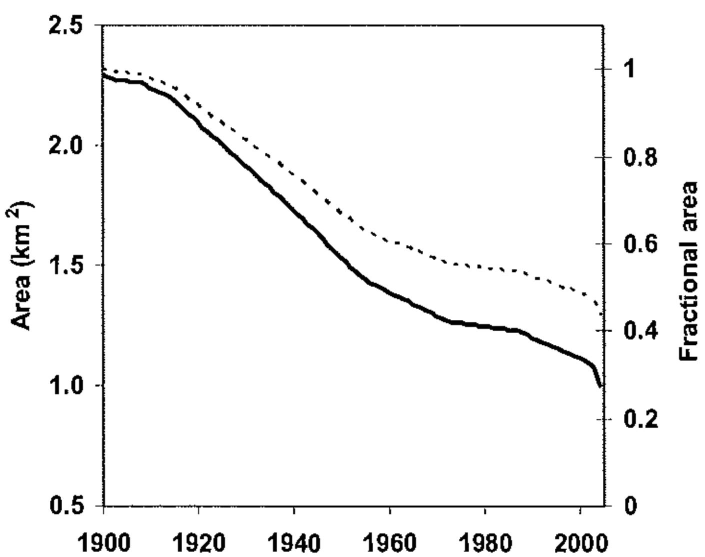

Figure 16. Total area change (solid) and fractional area change for the seven glaciers using a linear interpolation between data points.

I synthesized a glacier record assuming the timing of advance and retreat for each of the seven glaciers was identical. I adjusted the sum fractional area change of the seven glaciers (Figure 16), which is an average of the seven glaciers, to match years showing consistent trends among the individual glaciers. These years included 1916, 1955, 1972, 2003, and 2004. I used 1987 and 2001 to fill the gap between the 1970s and 2000s. The outcome of the adjustments represents the general pattern of glacier change in the Sierra Nevada (Figure 17). Four phases emerge from the synthetic construction. The first phase, between 1900 and 1920, indicate glacial stability. The glaciers rapidly retreat after 1920 until the 1950s. In phase III, early-1960s to mid-1980s, the glaciers stabilize and slightly advance. In the last phase beginning around 1985, the glaciers begin to retreat. The retreat rates increase in the early-2000s.

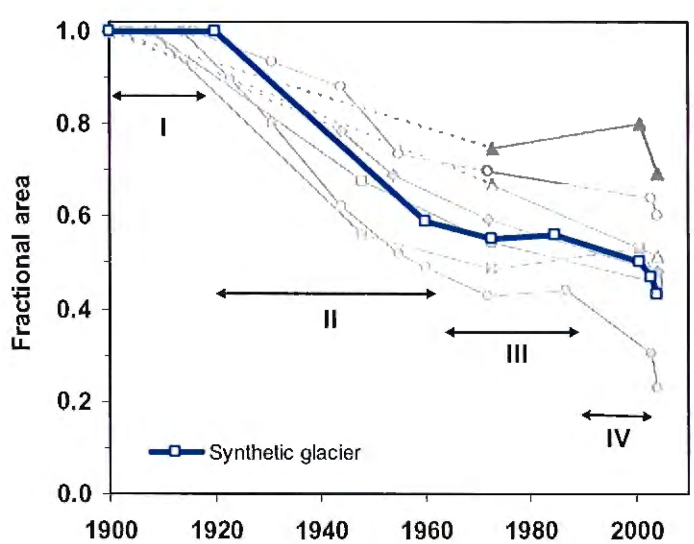

Figure 17. Fractional glacier area of the synthetic glacier over the past century. Horizontal arrows highlight four phases of glacier change (I – IV).

I extrapolated the changes of the seven glaciers to estimate the change for the glacier population in the Sierra Nevada assuming that the seven glaciers are representative of the glacier population and my depiction of the seven glaciers in 1972 is representative of the map-based inventory (1975 -1984). I applied the average fractional change of the study glaciers to the glacier population, to obtain area estimates for the population in 1900 and 2004. I used a 41% ($\sigma = 12\%$) area loss for 1900 – 1972, and an 18% ($\sigma = 14\%$) loss in area for 1972 – 2004. I calculated uncertainty by combing the uncertainty of the population (± 7.52) with the standard deviation of the percent change (12 and 14%). I estimate the 1900 population area was 66.36 ± 8.87 km^2 and by 2004 was 32.10 ± 9.31 km^2 in 2004, for a total area loss of 34.25 ± 12.85 km^2 between 1900 and 2004 (Table 8).

Table 8. Total glacier area (km^2) of the glacier population estimated for 1900 and 2004 based on the seven study glaciers and the map-based population inventory.

Year	Total area (km^2)	
1900	66.36	± 8.87
1972	39.15	± 7.52
2004	32.10	± 9.31
Area change (1900-2004)	-34.25	±12.85

5. CLIMATE ANALYSIS

Introduction

In this chapter I compare climate records to my observed glacier changes in order to infer which climate variables are important in controlling glacier change. I focus on air temperature and precipitation. Summer air temperature is important to melt and warmer temperatures provide more energy for melt. Winter air temperature is important to snow accumulation, as it determines the phase (snow versus rain) of precipitation. Winter precipitation in the form of snow is the source of mass to the glacier.

Methods

I used monthly temperature and precipitation data from the Parameter-elevation Regressions on Independent Slopes Model (PRISM), a spatially modeled dataset interpolated from surrounding stations for the years 1885 – 2004 (Daly et al., 1997). Several errors exist in the PRISM dataset which vary in magnitude and by location. The PRISM dataset is inconsistent in the southern Sierra Nevada because of new stations introduced in the late-1940s caused the precipitation and temperature records to change abruptly. These artifacts are a known issue in the data (Duly, personal communication). Therefore, I used data from a single grid cell (4km resolution) centered over Lyell Glacier, located at 37.743° N, 119.268° W, and elevation: 3512 m, for my climate analysis.

I also examined changes in spring snowpack because it is also sensitive to both temperature and precipitation. Long-term snow measurements are made on April 1, when snow accumulation is typically greatest (Cayan, 1996) at Dana Meadows (37.8970°N, 119.2570°W; 2988m elevation). This site was selected because it had a long history of measurements (1926 to present) and it is located at a high elevation close to glaciers.

Results

Climate trends

The mean annual air temperature increased by 0.6 °C ($r^2 = 0.06$, $p < 0.05$) over the past century (Figure 18). Seasonal spring (April – May), summer (June – September), and winter (November – March) mean temperatures all increased during the same period and were generally in phase with the annual mean temperature. Spring mean temperatures increased the greatest, + 1.8°C ($r^2 = 0.14$, $p < 0.05$). Summer and winter temperature increased by + 0.4°C (summer $r^2 = 0.03$, $p<0.05$; winter $r^2 = 0.01$, $p<0.05$). There was no trend for mean fall (October) temperatures. The mean spring, summer, and winter mean temperatures for the period were 0.2°C, 8.8°C and -5.4°C, respectively. There are several cool periods relative to the annual and seasonal means in 1910s – early 1920s, mid 1940s – mid 1950s, and mid 1960s – mid 1970s. Relatively warm periods occurred in the mid 1920s – mid 1940s, late 1960s, and the mid 1990s through the end of the record. The 25-year trends for annual temperature indicate a slight decrease for the first quarter (1901 – 1925), decreasing trends for two middle quarters (1926 – 1950 and 1951 – 1975), and a strong increase in temperature for the last quarter (1976 – 2000) (Figure 19). The 25-year trends for spring, summer, and winter were similar, but varied in slope.

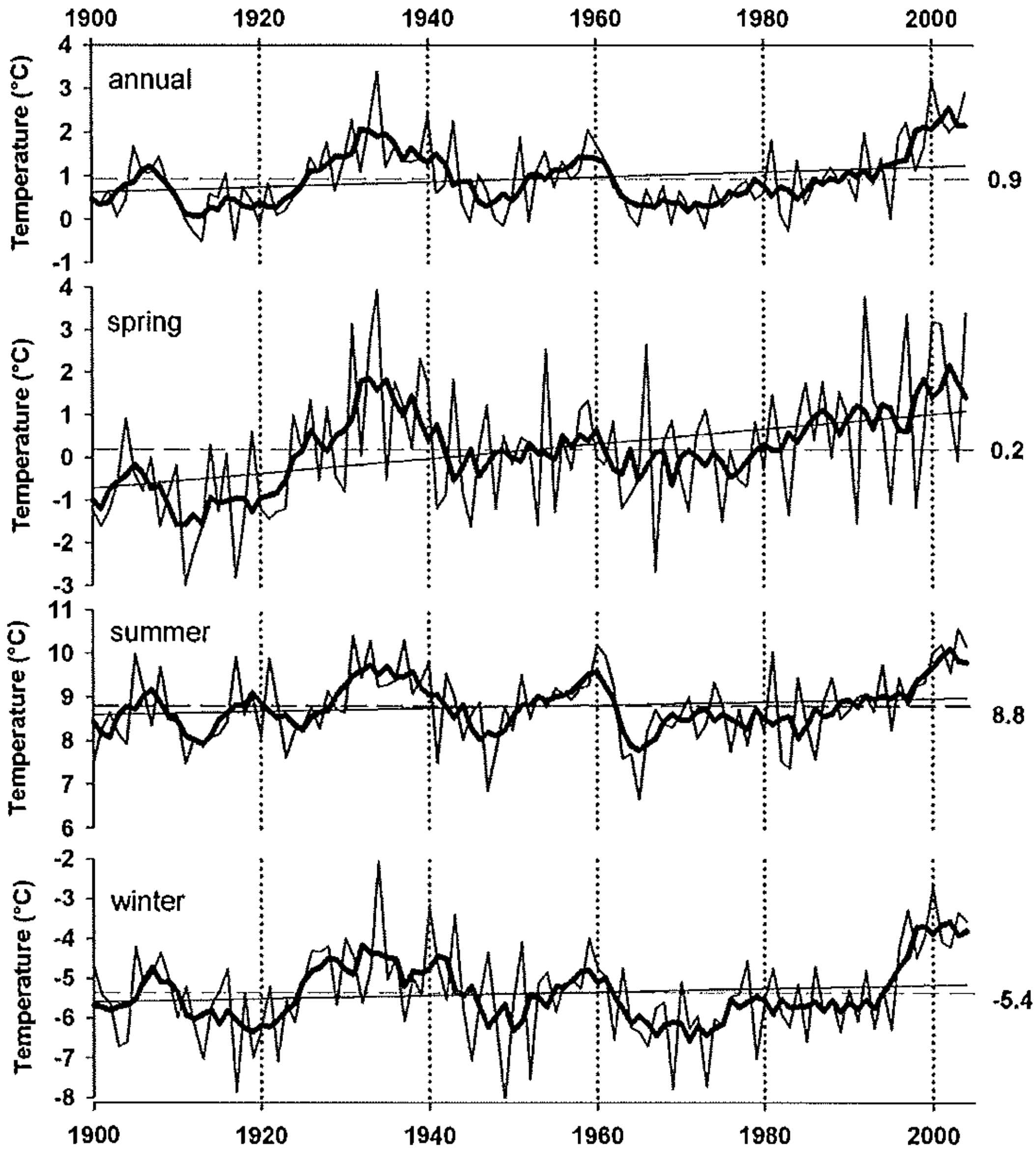

Figure 18. Mean temperature for (a) annual (Oct – Sept), (b) spring (April – May), (c) summer (Jun – Sept), and (d) winter (Nov – Mar) indicated by grey lines for the years 1900 – 2004. Trend line is given for 5 year running mean (thick black lines). Mean seasonal temperature for period shown with dashed grey line.

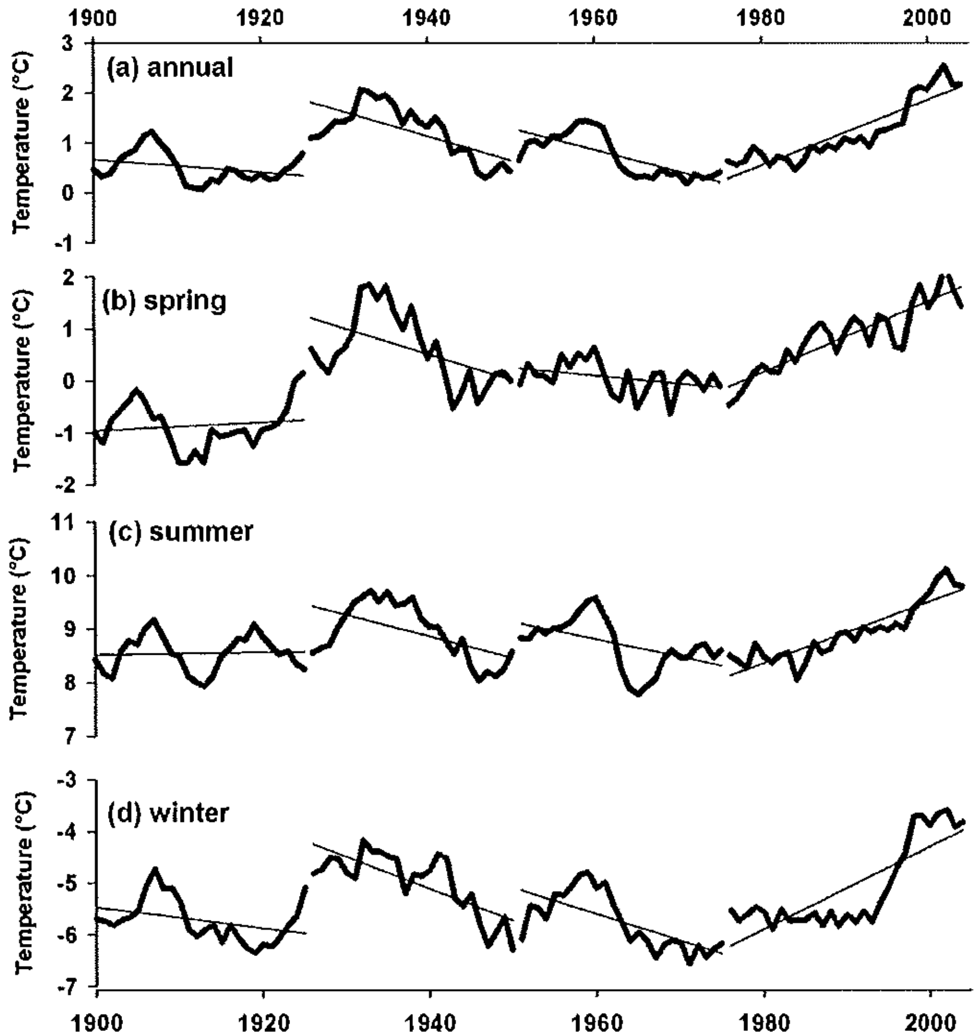

Figure 19. Linear trend lines for 25-year time periods for (a) annual, (b) spring, (c) summer, and (c) winter mean temperatures. Trends are based on 5-year running means.

The winter (November – March) precipitation record during the 20th century exhibited high annual variability (Figure 20). Winter precipitation was above the century mean (155.1 mm) for the periods of 1905 – 1914, 1936 – 1944, and 1978 – 1986, and below century mean periods occurred between 1920 – 1933, 1946 – 1950, 1957 – 1964, 1970 – 1977, and 1987 – 1993. There were three notable large snow years in 1907, 1938, 1969, and 1983 (>245 mm); and 1976 and 1977 winter precipitation was especially low (56 mm).

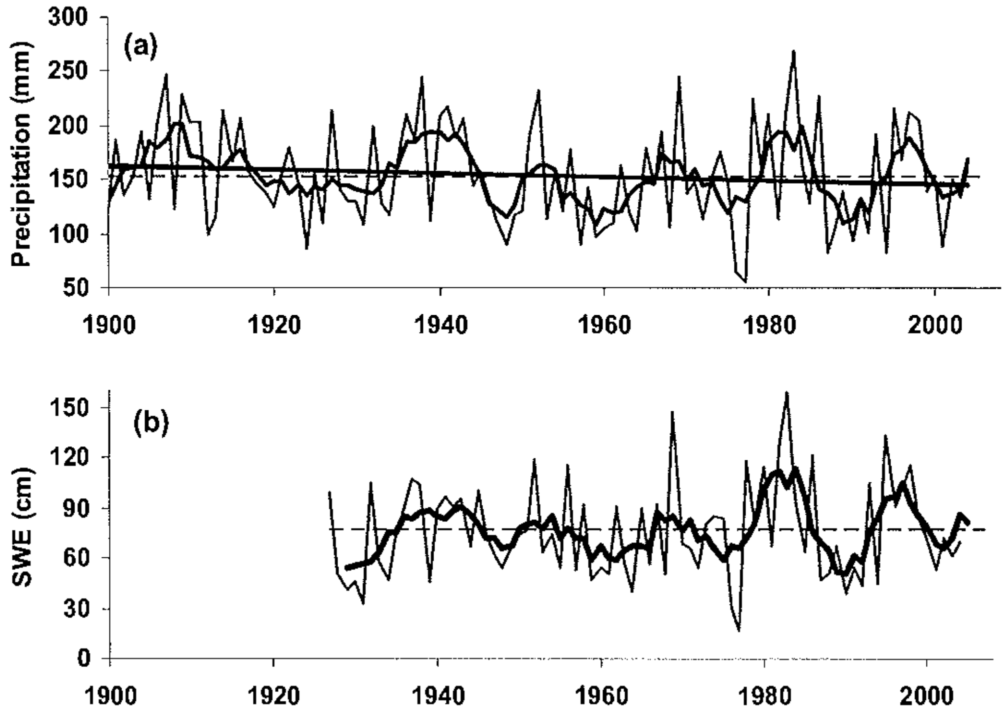

Figure 20. Winter (Nov – Mar) monthly mean precipitation (a) and (b) April 1st snow water equivalency (SWE) measured at Dana Meadows snow course. Annual data in grey and a running 5 year mean in black. The dashed grey lines represent mean values for winter precipitation (155.1mm) and SWE (76.4 cm) for the period of records.

The mean winter precipitation decreased slightly, by 14.9 mm ($r^2 = 0.04$, $p<0.05$), over the past century (Figure 20). The 25-year winter precipitation trends showed a 36mm increase for the 1901 – 1925 period ($r^2 = 0.35$, $p<0.05$). No trend occurred for the other three 25-year periods between 1925 and 2000. However, the mean monthly winter precipitation for the 1950 – 1975 period was about 10 mm lower compared to the other periods (Figure 21).

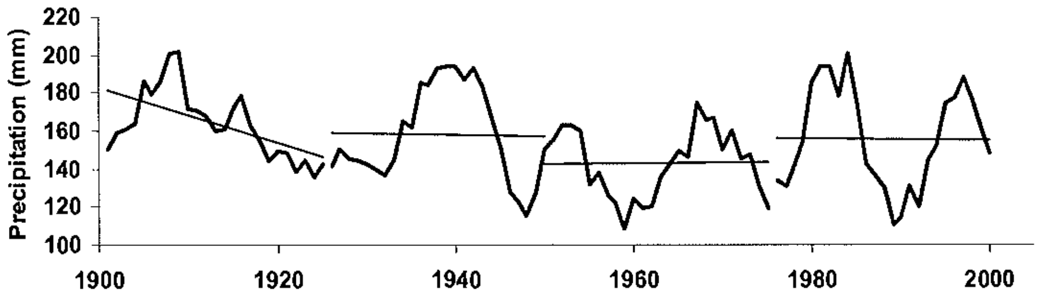

Figure 21. Winter (Nov - Mar) precipitation trends for 25-year time intervals over the 20th century.

Annual variability in snowpack data was similar to winter precipitation (Figure 20). Periods of above and below April 1st mean snow water equivalent, or SWE, (76 cm) match those of winter precipitation (above: 1935 – 1946, 1977 – 1983, and 1991 – 2001; below: 1929 – 1935, and 1984 – 1988). Notable high SWE years occurred in 1983, 1969, 1995, and low SWE years in 1976 and 1977. The 50-year trend in SWE at Dana Meadows, an increase of 13 cm WEQ, is consistent with the 50-year trend reported in the Sierra Nevada (Howat and Tulaczyk, 2005; Mote et al., 2005).

I compared variations in temperature and precipitation with hemispheric climate indices, using Pacific Decadal Oscillation (PDO) and El Niño Southern Oscillation (ENSO) data. PDO is defined by sea surface temperature in the North Pacific Ocean and persists for 20 to 30 years (Mantua et al., 1997). The PDO's regional affect on the Sierra Nevada climate is less than the Northwestern US (Cayan et al., 1998). "Cool" phases are typically marked by cooler air temperatures and above average precipitation in the Sierra Nevada. "Warm" phases are marked by warmer air temperatures and below average precipitation. Four distinct PDO phases occurred over the past century (<1925; 1925 – 1944; 1945 – 1976; >1976). These periods are similar to the 25-year trend analysis (Figure 22). Seasonal air temperatures, especially spring, are generally in phase with the PDO. Precipitation is more variable at shorter time intervals and is generally in phase with PDO since the 1930s.

ENSO events are defined by sea surface pressure in the central tropics of the Pacific Ocean and persist for 6 to 18 months. El Niño (warm) events typically produce above average precipitation in the Sierra Nevada. The counterpart La Niña events, while less significant in the Sierra Nevada, result in below average precipitation (Cayan et al., 1999). I plotted ENSO index data (NOAA, 2006) for the past 50 years to compare the index to winter precipitation and snowpack (Figure 22). There is high short-term variation in ENSO. Major El Niño events correspond to above average precipitation and snowpack, and vice versa, but the coincidence is not consistent.

Glacier-climate comparison

I expect glaciers to increase in area when spring and summer air temperatures are low and winter precipitation is high, and to decrease when conditions are reversed. I compare the four phases (I- IV) of my synthetic glacier to the three climate variables (Figure 23). Glacier area was constant during the cool/wet period in the early part of the century (phase I), before rapidly shrinking started in the 1920s as climate conditions became warm and dry (phase II). The glaciers continued to retreat rapidly through the late 1950s warm/dry period. The brief 1960s cool/wet period and the cool/wet years in the early 1980s bracket a period of below average temperatures. During this phase, the glaciers slowed and/or advanced. The glaciers resumed retreating by the late 1980s and accelerated retreat by 2001.

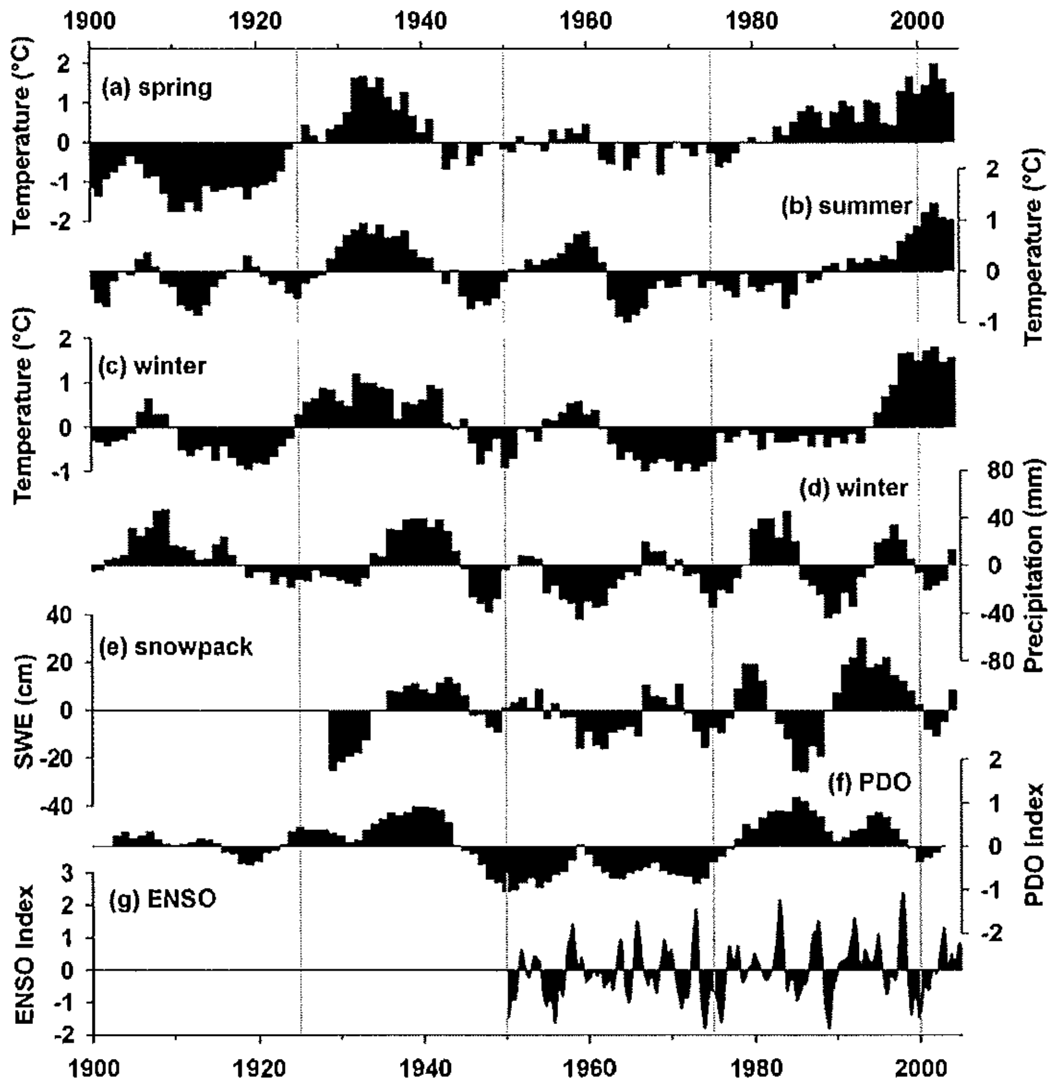

Figure 22. Climate summary with deviations from the mean monthly temperature for (a) spring, (b) summer, (c) winter; (d) mean monthly winter precipitation, (e) April 1 snowpack, (f) PDO for the past century, and (g) monthly ENSO index. All data is smoothed using a 5-year running mean, except for ENSO.

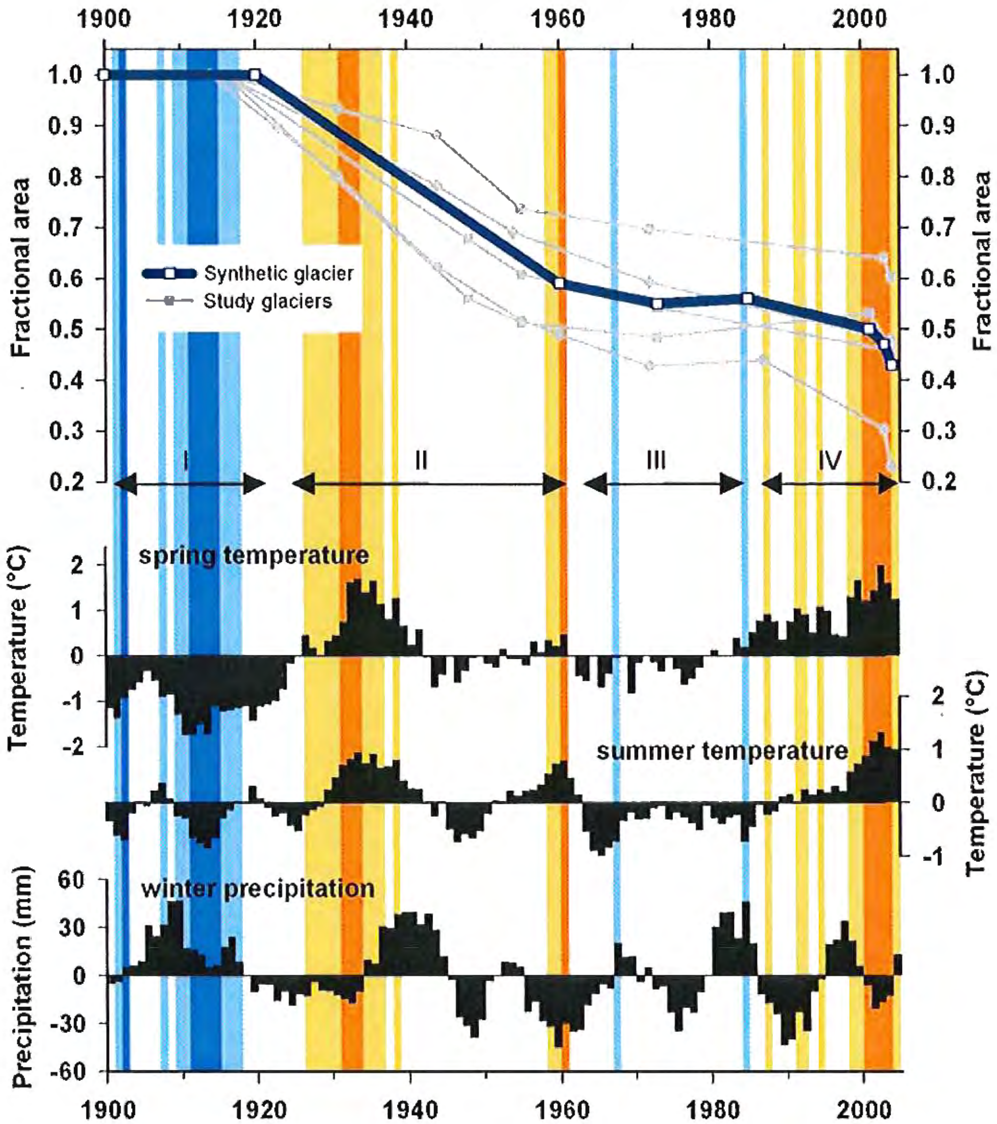

Figure 23. A comparison between fractional area change of the synthetic glacier (top) and three climate variables (black bars on bottom) over the past century. Horizontal arrows highlight the four glacier change phases. Climate variables are scaled as deviations from the respective means. Orange colors indicate above mean temperatures and below mean precipitation, blue colored bars represent the opposite. Light shaded bars indicate two of three climate variables >1 σ of the mean, while darker bars indicate all three variables exceed >1 σ of the mean.

The timing of the glacier phases appear to coincide with air temperature changes, especially spring (Figure 23). Winter precipitation varies on shorter time scales than air temperature and appears to have little effect on glacier activity. Glacier phase I ends after spring temperatures increase and winter precipitation decreases. Phase II is dominated either warm or average spring temperatures. Summer temperatures follow a similar pattern but exhibit larger fluctuations. Phase III is characterized by cool spring and summer temperatures. Phase IV is characterized by increasing spring and summer temperatures. The change from phase I to II coincides with the PDO phase changes from 'cool' to 'warm' PDO conditions. The other glacier phases did not coincide with PDO phase changes.

I compared temperature and precipitation variations to changes in glacier area by summing all the monthly mean temperature values above 0°C for each spring (March – May) and for summer (June – September) within the interval. This calculates a cumulative degree-month and allowed me to match the irregular intervals between the glacier data. I summed the monthly mean precipitation for the winter months (November – March) within interval of the glacier data. The temperature and precipitation data were compared to the glacier records for the East and West Lyell glaciers, and the synthetic glacier because they contain the greatest number of observations, 12, 8, and 8 respectively. Results (Table 9) show spring and summer temperatures are highly correlated with the area of East and West Lyell glaciers. Results comparing total winter precipitation and glacier area were statistically insignificant ($p<0.05$) for all glaciers.

Table 9. Regression results (r^2) for glacier area and climate variables. SpT = spring temperature, SuT = summer temperature, P = winter precipitation. Significant values are shown in bold ($p<0.05$).

Glacier	SpT	SuT	P
East Lyell	**0.87**	**0.61**	0.17
West Lyell	**0.90**	**0.78**	0.41
synthetic	**0.92**	0.48	0.52

I examined the frequency of positive degree-months for spring air temperatures because of the significant regression results. The degree-month totals for March and April show an increased frequency of positive degree-months (Figure 24). Positive degree-months for March have only occurred for 1934, 1997, and 2004, with the largest in 2004. Warmer spring air temperatures increase the duration of the melt season and consequently glaciers melt more. These results support the idea that the melt season is becoming warmer and longer in duration. However, the time interval of glacier data may bias against correlations with precipitation. Variations in precipitation are cyclic at time intervals shorter than the data frequency of my glacier data. Therefore a correlation between the two may not be observed if present. The poor statistical results between winter precipitation and area change may indeed be from the dominance of spring and summer air temperature on ablation in controlling glacier mass change, and thus area change.

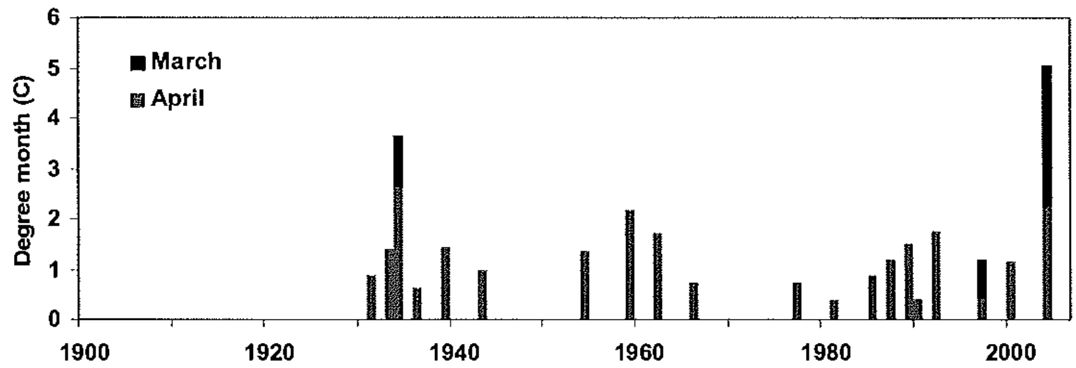

Figure 24. Total positive degree-months for March and April calculated for Lyell Glacier.

6. TOPOGRAPHIC ANALYSIS

Introduction

All Sierra Nevada glaciers have become smaller over the past century but have done so at different rates. Given that the temporal variation in climate is spatially uniform over the region, the variation in glacier response suggests that secondary factors influence glacier change. One secondary influence may be the glacier geometry. A thin glacier on a flat slope will lose more area compared to a thick glacier in a bowl-shaped depression with the same mass loss. Examination of the glacier profiles inferred from Equation (1) does not suggest any obvious difference that might lead to different retreat rates. The other secondary factor considered is local climate differences. Local topographic features such as mountain ridges and cirque headwalls modify regional climate by blocking incoming solar radiation, and enhance snow accumulation thorough avalanching and deposition of wind blown snow (Graf, 1976). Many small glaciers require these topographic conditions because the entire glacier exists below the theoretical snow line (Kuhn, 1995). In regions where glaciers are restricted to topographically protected areas, small differences in topography can explain the presence or absence of glaciers (Allen, 1998). For example, a cirque basin can control patterns of incoming shortwave solar radiation, important to the morphology and development of cirque glaciers (Chueca and Julian, 2004) and ultimately glacier shape (Graf, 1976). Kuhn (1995) notes that wind can enhance accumulation by a factor of 2 on small cirque glaciers and avalanching can increase by a factor of 4. Mass balance measurements at Maclure Glacier in 1967 indicated that redeposition of winter snow from the surrounding area contributed 43% of total accumulation (Tangborn et al., 1977).

The magnitude of topographic control can change through time (Graf, 1976; López-Moreno et al., 2006). A glacier that extends outside of a cirque basin is less affected by cirque topography than one confined within the basin. Glaciers of the Sierra Nevada currently occur at the base of steep headwall cliffs. Clark and Gillespie (1997) suggest these glaciers have become increasingly dominated by local topographic conditions as they have become smaller.

Local topography is important to glacier mass and surface energy exchanges of alpine glaciers (Figure 1). Topographic variables, such as elevation, slope, aspect, and cirque headwall cliffs can influence one or more of the surface energy balance components. The glacier surface energy balance can be summarized (Paterson, 1999) as,

$$0 = (1 - \alpha)\, Q_{SW} + Q_{LW} + Q_H + Q_L + Q_m \qquad (3)$$

where, Q_{SW}, is incoming shortwave radiation, α is the surface albedo, Q_{LW}, is the net (incoming minus outgoing) longwave radiation, Q_H and Q_L, are sensible and latent turbulent fluxes, respectively, and Q_m, is energy consumed by melt or released by freezing. The topographic variables affect the energy balance by reducing the incoming shortwave radiation through shading.

I examined the topographic effect on glacier retreat in three sections. Specifically, I summarize topographic characteristics of the study glaciers, compare the topographic factors to glacier area change to determine if they explain the variation in change between glaciers, and examine three environmental variables to define the environmental conditions in which they retreated.

Topographic characteristics

I calculated four topographic characteristics for each of the 14 study glacier's 2004 glacier boundary. I used a zonal statistic to average the elevation, slope, and aspect at each glacier, using a 10 m DEM. An inherent problem with this analysis is that elevation data DEM are based on 1975 -1984 data while my glacier boundary was established in 2004. I was unable to correct the elevation data. Differences in elevation influence my results, but the elevation error is small because the glaciers are thin at the terminus indicating a 10 to 20 m difference between dates.

I measured the mean cirque headwall height above each glacier by taking the elevation difference of the peak or ridge above the glacier and the 2004 glacier boundary at the base of the wall based on the DEM. I averaged three to four elevation pairs depending on the length of headwall.

The elevation, slope, and aspect of the 14 study glaciers in 2004 (Table 10) were similar to the glacier population database (Chapter 4, Table 3), although mean elevation increased by 19 m and mean slopes steepened by 3°. The small differences were from changes in glacier area between the map used for the population and the 2004 and differences in methodology, as described in Chapter 4. Headwall cliffs above the glaciers ranged in height between 44 m at East Lyell Glacier to 305 m at Brewer Glacier, with an average of 173 m. In 2004, East Lyell Glacier had separated into two smaller lobes under separate cirques. I combined the results to allow for comparison with historical conditions.

Table 10. Spatial and topographic variables for 14 glaciers based on 2004 glacier extents, except where noted (2003 = *, 2005 = **, 2006 = ***) Elv = elevation (meters), Slp = slope (°), Asp = aspect (°), HW = headwall height (meters), area change = area change 1900-2004 (%).

Glacier	Latitude	Longitude	Glacier area (m^2)	Elv	Slp	Asp	HW	Area change (%)
Dragontooth	38.1000	-119.3838	54788***	3419	38	7	162	-74
Conness	37.9695	-119.3192	159965	3660	26	16	171	-52
Dana	37.9013	-119.2173	179409	3569	30	30	190	-44
Maclure	37.7465	-119.2806	155300*	3707	27	352	165	-47
West Lyell	37.7439	-119.2640	279492	3794	22	357	85	-39
East Lyell	37.7430	-119.2722	140285	3707	30	3	44	-78
Darwin	37.1712	-118.6768	117173	3882	33	359	238	-54
M. Goddard	37.1091	-118.7129	34680	3721	35	5	155	-69
Goddard	37.1075	-118.7030	173389	3742	31	358	153	-54
Black Giant	37.1056	-118.6470	68800	3640	37	48	305	-39
M. Palisade	37.0751	-118.4679	173462**	3792	31	38	261	-44
Brewer	36.7100	-118.4820	145555**	3832	35	16	123	-71
Lilliput	36.5723	-118.5532	48464	3373	34	336	261	-31
Picket	36.5593	-118.5082	79835	3660	26	16	113	-49

My results show shrinkage with increasing latitude and with westerly longitudes (Figure 25). The relationships for both latitude and longitude are weak (r^2 = 0.05, and 0.04) and statistically insignificant (p= 0.50). The trend in latitude may be confounded by the decreasing trend in elevation with increasing latitude. Similarly, the trend in longitude may be confounded by the grouping of glaciers (Figure 25) in areas separated by the low elevation river valley region of the Middle Fork of the San Joaquin River.

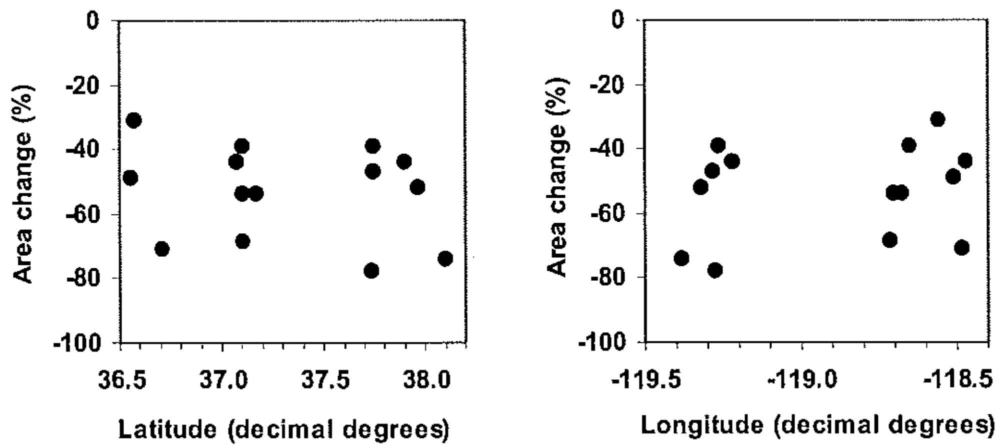

Figure 25. Glacier area change (1900 – 2004) as a function of latitude and longitude.

Results comparing the topographic variables of elevation, slope, and aspect to area change were also poor and statistically insignificant ($p<0.05$) (Figure 26). A slight increase in area shrinkage is observed with increased elevation ($r^2 = 0.03$). An increase in area loss was observed with increasing slope ($r^2 = 0.10$). No trend was observed with aspect. The headwall height shows the strongest relationship with area change ($r^2 = 0.32$) and was significant ($p < 0.05$). In general, glaciers with higher headwall cliff experience less glacier area loss. The other topographic variables, while not important alone, are likely important in combination with other variables. I was unable to test this with a multiple linear regression because I was limited by my sample size of 14 glaciers.

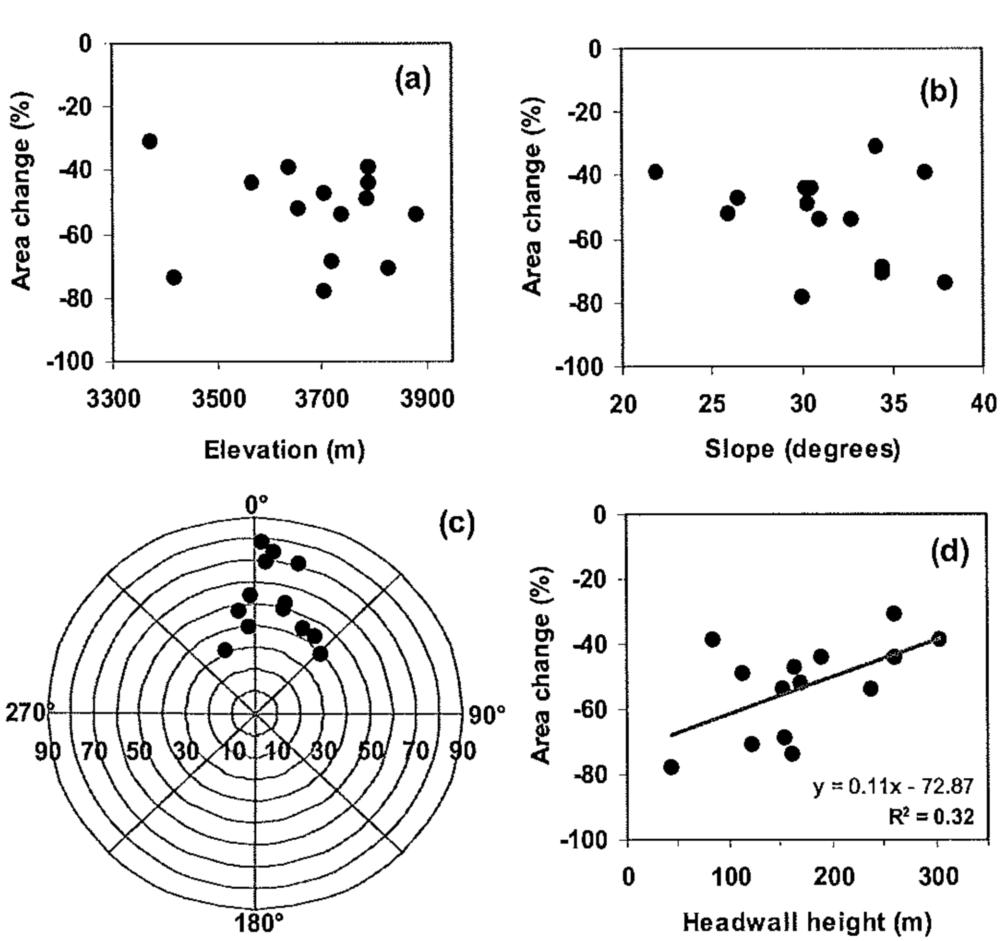

Figure 26. Glacier area change (1900 – 2004) as a function of (a) elevation, (b) slope, (c) aspect, and (d) mean headwall cliff height above glacier. The concentric circles on (c) indicate percent loss, so that the outer circle equals 90% area loss.

Change in mean glacier conditions

I examined three environmental variables to determine if glaciers have retreated into more favorable environmental conditions through time. These variables include solar radiation, elevation, and the ratio between headwall cliff area and glacier area. I used the ArcView Solar Analyst extension (Fu and Rich, 2002) to calculate the total annual magnitude of incoming solar radiation, or insolation (direct + diffuse radiation) for each of the 14 study glaciers. Solar Analyst calculates insolation based on an elevation model and accounts for changes in viewshed, surface orientation, elevation, and atmospheric conditions. I assumed clear skies to identify differences in potential annual insolation. Solar radiation was calculated for glacier configurations in 1900 and 2004 to determine change in annual insolation and summarized with an area weighted mean.

The total mean annual insolation decreased for all 14 study glaciers over the past century by an average of 15 W m^{-2} (Figure 27). Dragontooth Glacier had the largest decrease in mean insolation, by 38 W m^{-2} (-28%). In contrast, West Lyell Glacier decreased the least, by 5 W m^{-2} (-3%). The mean elevation of the 14 study glaciers increased an average of 38 m, equivalent to -0.2°C based on an environmental lapse rate of 6.5°C km^{-1}. Conness Glacier experienced the largest change in mean elevation (110 m) corresponding to a -0.7°C temperature change. The mean elevation increased for all glaciers except Darwin, which decreased by 2 m because of unusual area loss over all elevations of the glacier. Overall, the results show that glaciers have retreated into cooler, more shaded, and higher in elevation locations.

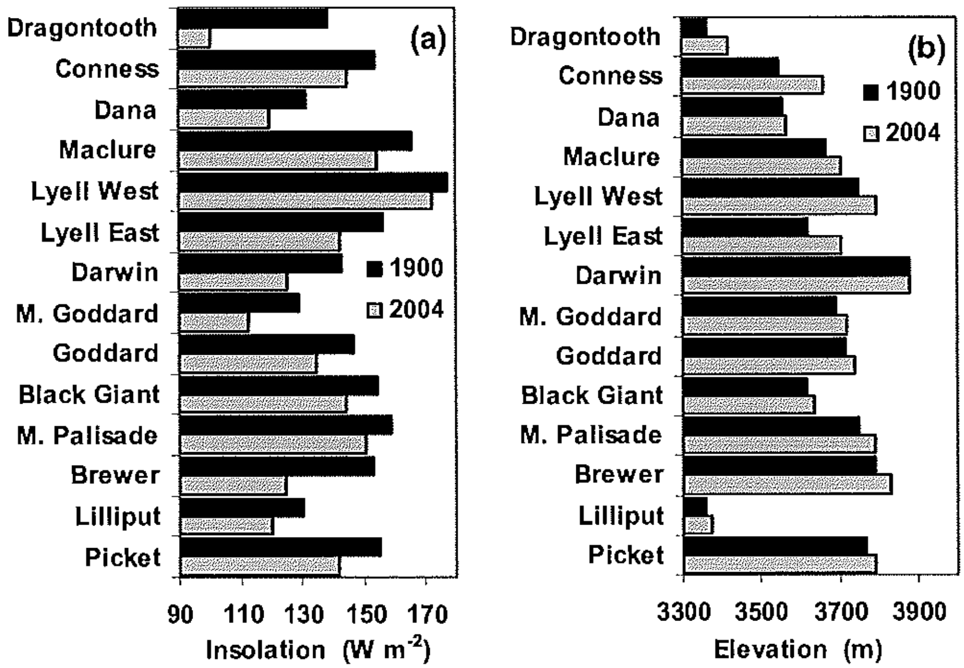

Figure 27. Mean (a) annual clear sky insolation (W m^{-2}) and (b) mean elevation (m) calculated at 14 glaciers for the 1900 and 2004 glacier areas.

I calculated the ratio between headwall cliff area and glacier area to estimate the potential contribution area of avalanched snow to the glacier. I used the seven study glaciers to estimate the potential contribution for three time periods: 1900, 1972, and 2004. The headwall cliff area was calculated in a raster based GIS. I derived the slope from a 10m DEM for the vicinity around each glacier and used ArcMap hydrologic modeling tools to determine flow direction and accumulation. A "flow direction" command calculated the greatest elevation drop between neighboring cells. I calculated flow direction for cells with slope angles > 40°. I used 40° as a conservative threshold as the mean critical angle for moderate slab avalanches (McClung and Schaerer, 2006). A "flow accumulation" command calculated the number of neighboring cells that flow into a cell. I used a series of conditional statement to extract flow accumulation values at the cell where the flow crossed the glacier boundary. I assume the snow stops and accumulates on the glacier, and that the contribution of the headwall cliff area remained the same through out the three time periods.

Headwall cliff area varies widely between glaciers (Figure 28). The ratio of headwall to glacier area also varied between glaciers from 2% at West Lyell Glacier to 200% at Lilliput Glacier. All ratios increased over the century because of the decrease in glaciers area. The ratio nearly doubled at most glaciers, except for East Lyell Glacier, which increased by 4 times, and Lilliput Glacier that increased by half. No statistical relationship was observed between headwall area and glacier area change.

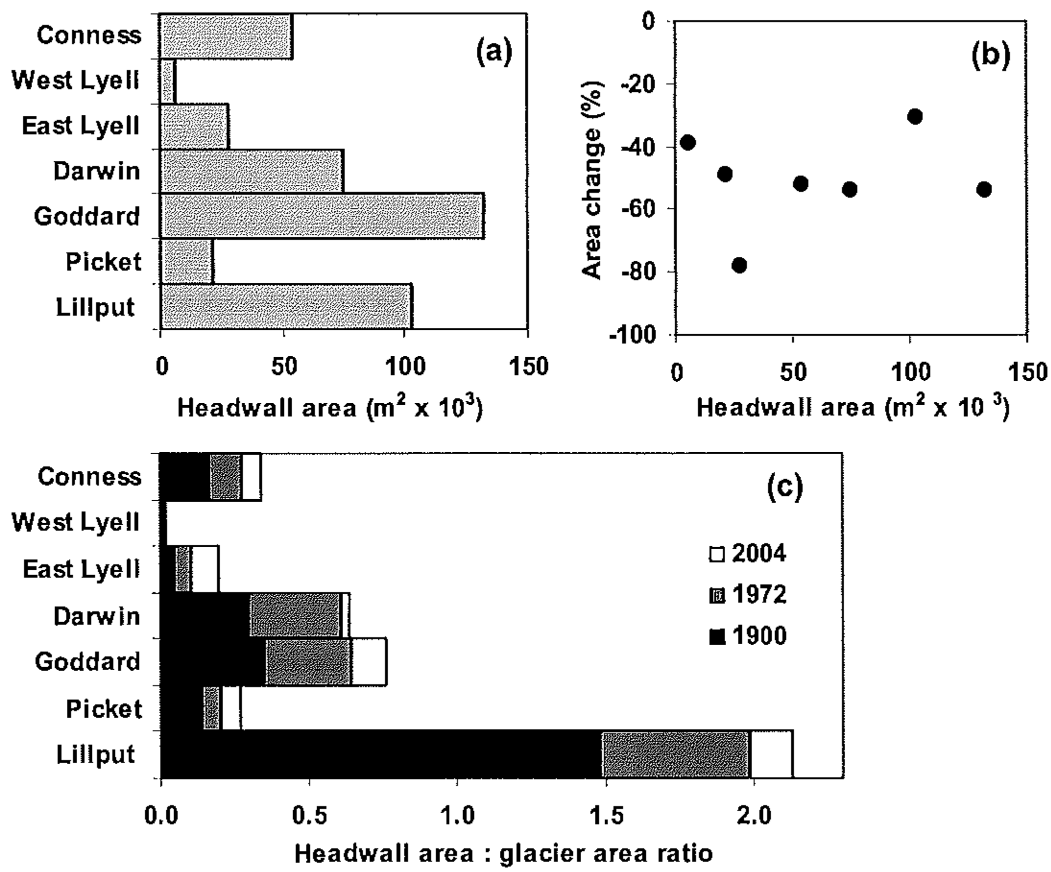

Figure 28. Headwall area (a) of the seven study glaciers, (b) headwall area with glacier area change, and (c) the ratio of headwall to glacier area for 1900, 1972, and 2004.

Case study at Lyell Glacier

I examined temporal changes in the three environmental variables at East and West Lyell Glaciers. These two glaciers have the best records over the past century and have different area responses. I calculated the mean temperature, insolation, and headwall cliff to glacier area ratio for each glacier record based on the boundary. I estimated temperature changes by applying an environmental adiabatic lapse rate (6.5°C km^{-1}) to the mean glacier elevation. Mean annual insolation results were summarized for each glacier record using zonal statistics. I used the area of each glacier record to calculate the changing headwall to glacier area ratio.

The Lyell case study results show that the environmental variables changed at different rates through time suggesting different responses for temperature, insolation, and ratio of headwall to glacier area (Figure 29). The dramatic loss of area at East Lyell is evident in all three plots. The elevation-dependent mean temperature at East Lyell decreased by -0.6° C, while the temperatures at West Lyell decreased by only -0.3°C. The temperature decrease at East Lyell matches the regional temperature increase of 0.6°C over the past century, while the temperature change at West Lyell is one half of the regional increase. Changes in insolation also varied between glaciers. East Lyell decreased by 14 W m^{-2}, and 6 W m^{-2} at West Lyell. Most insolation changes at East Lyell occurred in the 1930s and 1940s, with little change after 1960 until recently. The rate of insolation change at West Lyell has remained steady over the past century. Headwall to glacier area ratio results are similar to insolation changes; East Lyell increased more, from 0.04 to 0.20, compared to West Lyell, from 0.01 to 0.02. The ratio at East Lyell increased from the 1910s to 1970s, when the rate of area loss paused through the mid 1980s and then increased sharply. The ratio at West Lyell has changed less, but has increased steadily except for an increase in 1940s and a more recent increase in 2000s. The underlying difference between the glaciers is caused by the greater area loss in East Lyell's lower portion as compared to West Lyell (Appendix E). The different area-altitude distributions caused East Lyell to lose much of its less shaded, lower elevation areas compared to West Lyell Glacier.

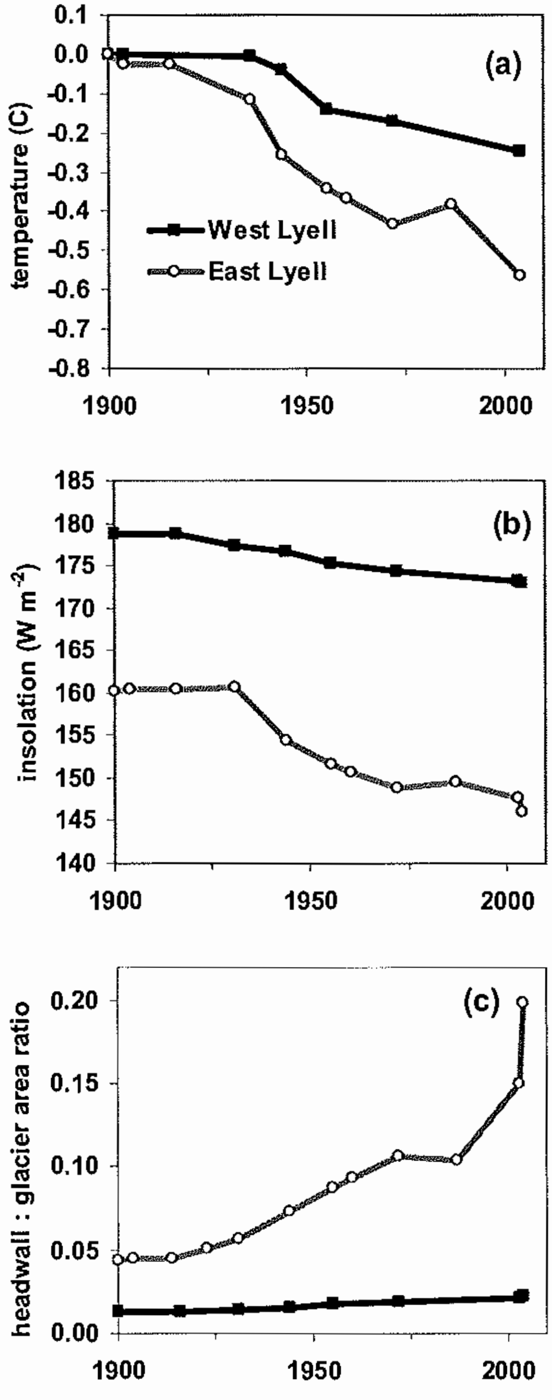

Figure 29. Calculated change in (a) temperature based on environmental lapse rate (6.5°C km^{-1}), (b) potential mean annual insolation, and (c) headwall to glacier area ration for East and West Lyell Glaciers over the 20^{th} century.

The topography of the Sierra Nevada affects the response of glaciers to regional climate. Cirque headwall cliff height had a significant ($p<0.05$) statistical relationship ($r^2 = 0.32$, $p<0.05$) to glacier area change, and showed that glaciers with higher headwalls changed less in area over the past century. These results suggest that headwall cliffs protected the glaciers by decreasing exposure to solar radiation and enhanced accumulation via avalanching. The poor results for other topographic variables may indicate that different combinations of variables affect glaciers in different ways, some of which reduce glacier retreat more than others, while other combinations may counter a glacier response. For example, Lilliput Glacier commonly appeared as an outlier because of its small area (0.048 km^2) with unique topographic characteristics that included a low mean elevation (3373m), a high headwall cliff height (261m), and a large headwall cliff area (0.103 km^2) to glacier area ratio (2.13). In contrast, the larger West Lyell Glacier (0.279 km^2) posses a different combination of topographic characteristics that include a high mean elevation (3794m), a small headwall cliff height (85m), and a small headwall cliff area (0.006 km^2) to glacier area ratio (0.02). The difference in mean elevation between the two glaciers is 421m, the equivalent of 2.7°C with an environmental adiabatic lapse rate (6.5°C km^{-1}) applied. The difference in cliff height and surrounding topography results in a more shaded Lilliput Glacier, which receives 52 W m^{-2} less annual insolation than West Lyell Glacier. The difference between cliff areas indicates that Lilliput Glacier has 17 times more area above that has potential for avalanching snow. The two glaciers have different topographic characteristics and different magnitudes of area change over the past century, Lillput Glacier with 0.02 km^2 and West Lyell Glacier with 0.18 km^2, but the two have similar fractional change, 31 and 38 % respectively. Lilliput Glacier appears to be more reliant on enhanced precipitation and shading to overcome the warmer temperatures. Frequent avalanching on Lilliput Glacier is apparent from large avalanche cones observed on the glacier.

The Lyell case study shows how changes in area can alter the mean glacier conditions. Differences in area loss is largely driven by differences in area-altitude distribution that created conditions at East Lyell that are cooler, more shaded, and dominated by the effects of cirque headwall. Conditions have also changed at West Lyell, where area loss has been slower, and the influence of local effects appears to be less. This analysis supports the hypothesis that, as glaciers have retreated over the past century, they have retreated to locations that are more controlled by local topography. Greater local topographic control may lessen the glacier area response to regional climate. This has implications on the interpretation to future glacier area changes.

7. DISCUSSION AND CONCLUSION

I identified a total of 1719 glaciers in the high elevation portions of the central and southern Sierra Nevada with a mean area of 0.02 ±0.04 km^2 and total area of 39.15 ±7.52 km^2. By comparison, Raub et al. (2006) found a total of 1344 glaciers using a hand drawn inventory for glaciers >0.01km^2. Filtering my inventory to the same size range yielded similar results despite the different methods and different photographic years. Comparison between inventories for 'true' glaciers was less satisfactory because of differences in definition. Earlier inventories counted 50 to 70 glaciers (Kehrlein, 1948; Meier, 1961) by defining glaciers with a size threshold (Meier, 1961; Raub et al., 2006) or requiring evidence of movement, such as the presence of a crevasse (Kehrlein, 1948; Raub et al., 2006). Differences in definition strongly influence the number of glaciers identified in the Sierra Nevada because the glaciers are small and near the threshold of any definition.

The magnitude of change for a subset of seven glaciers since 1900 ranged from 31% to 78%, an average of 55%. If applied to all glaciers in the Sierra Nevada the total area loss would be 34.25 ± 12.85 km^2. The rate of change was categorized into four phases. In the first phase glacier area was constant from 1900 to about 1920. Phase II marked a rapid retreat from about 1920 through the 1950s. In phase III, the retreat slowed and in some cases the glaciers advanced. Phase IV began in the mid-1980s when glacier began retreat, and increased its rate of retreat in the early 2000s.

This pattern is similar to other glacier regions in the Western US and the world. Glaciers in the Wind River Range, Wyoming lost 42% area over the past century (DeVisser, unpublished), and those in the Front Range, Colorado lost 40% (Hoffman et al., 2007). In the Trinity Alps of California, the glaciers lost 10 to 20% of their area between 1950 and 2000 (Heermance and Briggs, 2005) during which time the Sierra Nevada lost about 30%. The Sierra Nevada lost more relative area than glaciers on Mount Hood, Oregon (34%) between 1901 to 2004 (Jackson and Fountain, 2007); than Mount Rainier, Washington (18.5%) between 1910 to 1994 (Nylen, 2004); and North Cascades National Park, Washington (7%) between 1958 to 1998 (Granshaw and Fountain, 2006). Only glaciers in Glacier National Park, Montana lost a greater area (65%) between 1850 to 1979 (Key et al., 1998; Hall and Fagre, 2003). Hoelzle et al. (2007) reported similar area change for glaciers in the Southern Alps of New Zealand, which lost 49% and in the European Alps, 35% between 1850 and 2006.

The temporal pattern of 20th century glacier retreat in the Sierra Nevada is similar to that throughout the Western US and world. The retreat – advance – retreat pattern is common for glaciers over the past century though variations in timing exist (Dyurgerov and Meier, 2000). Most glaciers, including those in the Sierra Nevada, began retreating in the 1920s -1930s. The retreat lasted until the late 1940s and early 1950s when most glaciers stabilized. By the 1960s the glaciers in the Northwest US began to advance (Hubley, 1956; LaChapelle, 1965). Glaciers in the European Alps continued to advance through the 1970s until a return to general retreat in the 1980s.

Most glaciers in the Northwest US returned to retreat in the 1980s and 1990s. The glaciers in the Sierra Nevada appear consistent with global glacier responses.
An exception are glaciers on Mount Shasta that advanced 1995 – 2003 (Howat et al. (2007). This difference is attributes to increased snowfall at higher elevations on Mount Shasta and is unique relative to all other monitored glaciers in the Western US.

The large decline in glacier area indicates an indirect influence of climate change over the past century. Historical glacier retreat in the Sierra Nevada occurred during extended periods of above average spring and summer temperatures. Comparisons showed that above average spring and summer air temperatures significantly correlated ($p<0.05$) with glacier area changes at East Lyell (spring $r^2 = 0.87$, summer $r^2 =0.61$) and West Lyell (spring $r^2 = 0.90$, summer $r^2 = 0.70$). Winter precipitation did not correlate well with glacier change, suggesting that either the interval between glacier data was insufficient or that air temperatures are dominating the glacier response. Hoffman et al. (2007) reached similar conclusions regarding glacial response in the Front Range, Colorado to spring and summer temperatures. They found winter accumulation was less important than spring and summer snow events which affected the length of melt season. Warmer spring air temperatures and earlier arrival of spring since the 1970s are consistent with the findings of Cayan et al. (2001) and Stewart et al. (2005) who reached a similar conclusions for spring snowpack runoff.

The variation in individual glacier response is caused in part by differences in local topography, particularly high headwall cliffs. Cliff height had the strongest correlation ($r^2 = 0.32$, $p<0.05$) among the topographic variables and glacier area change. Headwall cliffs reduce solar insolation and enhance snow accumulation through avalanching.

Implications

Given the current climate conditions glaciers are likely to continue retreating but the rate may be dampened by the effects of local topographic influences. The increasing topographic dominance makes projecting future glacier changes difficult as future climate influences may be locally mitigated. The current retreat rate for the 1972 – 2004 period ranges from 0.0001 to 0.0038 $km^2\ yr^{-1}$, a mean of 0.0012 km^2 for a subset of glaciers. These values, if constant, indicate these glaciers will disappear in 250 years, ±200 years.

The loss of glacier area has implications for the local alpine hydrology. The glacier's ability to act as a frozen reservoir will decrease, diminishing the ability to buffer ponds and streams, thereby exposing them to increasing summer droughts (Fountain and Tangborn, 1985). Flora and fauna depend on available water resources and have adapted to these conditions. Changes in vegetation have already been documented in sub-alpine fur trees (Millar et al., 2004) and for small mammals (Conroy et al., 2006) in the Sierra Nevada.

Suggestions for future work

The most valuable information on Sierra Nevada glaciers would be to obtain volume change estimates. Volume measurements would quantify changes that area measurements alone miss, and could be more directly related to changes in climate. Increasing the number of study glaciers and interval between observations would improve statistical analyses presented in the climate and topographic analysis chapters of this thesis. I recommend the continuation of repeat photography and GPS mapping of glacier terminus as an important and cost-effective method of documenting change. Monitoring should be conducted at a minimum of every 5 years. Additionally, I recommend an updated glacier inventory to fully document change throughout the entire range.

8. REFERENCES CITED

Allen, T. R. 1998. Topographic context of glaciers and perennial snowfields, Glacier National Park, Montana. *Geomorphology*, 21:207-216.

Antevs, E. 1938. Post-pluvial climatic variations in the Southwest. *Bulletin of the American Meteorological Society*, 19(190-193).

Beatty, M. E. 1939. Yosemite National Park Glacier Measurements: 1939 Report, National Park Service. Yosemite National Park. 42 p.

Benson, L. V., Burdett, J. W., Kashgarian, M., Lund, S. P., Philips, F. M. and Rye, M. O. 1996. Climatic and Hydrologic Oscillations in the Owens Lake Basin and Adjacent Sierra Nevada, California. *Science*, 274(5288):746-749.

Birman, J. H. 1964. Glacial geology across the crest of the Sierra Nevada, California. *Geological Society of America Special Paper*, 75:1-80.

Blackwelder, E. 1931. Pleistocene glaciation in the Sierra Nevada and Basin Ranges. *Geological Society of America Bulletin*, 42:865-922.

Bowerman, N. D. 2006. Holocene Glaciation of the Central Sierra Nevada, California. Masters Thesis, Geology Department, Western Washington University, Bellingham, WA: 65 p.

Brittain, J. E. and Milner, A. M. 2001. Ecology of glacier-fed rivers: current status and concepts. *Freshwater Biology*, 46(12):1571-1578.

Cayan, D. R. 1996. Interannual climate variability and snowpack in the western United States. *Journal of Climate*, 9:928-948.

Cayan, D. R., Dettinger, M. D., Diaz, H. F. and Graham, N. E. 1998. Decadal climate variability of precipitation over western North America. *Journal of Climate*, 11/12:3148-3166.

Cayan, D. R., Kammerdiener, S. A., Dettinger, M. D., Caprio, J. M. and Peterson, D. H. 2001. Changes in the Onset of Spring in the Western United States. *Bulletin of the American Meteorological Society*, 82(3):399-415.

Cayan, D. R., Redmond, K. T. and Riddle, L. G. 1999. ENSO and Hydrologic Extremes in the Western United States. *Journal of Climate*, 12(9):2881-2893.

Chambers, F. 1992. Mass balance and cold air ponding, an analysis of Conness Glacier. *Eos Trans. American Geophysical Union, Fall Meeting*, 73:180.

Chen, J. and Ohmura, A. 1990. Estimation of alpine glacier water resources and their change since the 1870s, Hydrology in mountainous regions - I. Hydrologic measurements, the water cycle, Proceeding of the two Lausanne Symposia. *IAHS Publ. no. 193*:127-135.

Chueca, J. and Julian, A. 2004. Relationship between solar radiation and the development and morphology of small cirque glaciers (Maladeta Mountain Massiff, Central Pyreness, Spain). *Geografiska Annaler*, 86 A(1):81-89.

Clark, D. H. and Gillespie, A. R. 1997. Timing and significance of late-glacial and Holocene glaciation in the Sierra Nevada, California. *Quaternary International*, 38/39:21-38.

Conroy, C. C., Koo, M., Monahan, B., Parra, J. and Moritz, C. 2006. The Grinnell Project; Small Mammal Responses to Climate in California. *Eos Trans. American Geophysical Union, Fall Meeting*.

Curry, R. R. 1969. Holocene climatic and glacial history of the central Sierra Nevada, California. *United States Contributions to Quaternary Research, Geological Society of America Special Paper 123*: 1-47 p.

Daly, C., Taylor, G. and Gibson, W. 1997. The PRISM approach to mapping precipitation and temperature. *10th Conference on Applied Climatology*, Reno, NV, American Meteorological Society.

DeVisser, M. unpublished. Twentieth Century Glacier Change in the Wind River Range, WY.

Dougall, J. A. 2007. Downstream Effects of Glaciers on Stream Water Quality. Masters Thesis, Geography, Portland State University, Portland, OR: 130 p.

Dyurgerov, M. B. and Meier, M. F. 2000. Twentieth century climate change: Evidence from small glaciers. *PNAS*, 97(4):1406-1411.

Farquhar, F. P. 1920. Photograph of Lyell Glacier. *Sierra Club Bulletin*, 11:Plate 23.

Fountain, A. G., Hoffman, M. J., Jackson, K. M., Basagic, H. J., Nylen, T. and Percy, D. 2007. Digital Outlines and Topography of the Glaciers of the American West: U.S. Geological Survey Open-File Report 2006–1340. 23 p.

Fountain, A. G., Krimmel, R. M. and Trabant, D. C. 1997. A strategy for monitoring glaciers. *U.S. Geological Survey Circular 1132*:1-19.

Fountain, A. G. and Tangborn, W. V. 1985. The effect of glaciers on streamflow variations. *Water Resources Research*, 21(4):579-586.

Fu, P. and Rich, P. M. 2002. A geometric solar radiation model with applications in agriculture and forestry. *Computers and Electronics in Agriculture*, 37:25-35.

Gilbert, G. K. 1904. Variations of Sierra Glaciers. *Sierra Club Bulletin*, v(1):20-25.

Graf, W. L. 1976. Cirques as Glacier locations. *Arctic and Alpine Research*, 8(1):79-90.

Granshaw, F. D. 2002. Glacier Change in the North Cascade National Park Complex, Washington USA, 1958 to 1998. Masters Thesis, Department of Geology, Portland State University, Portland, OR: 134 p.

Granshaw, F. D. and Fountain, A. G. 2006. Glacier change (1958-1998) in the North Cascades National Park Complex, Washington, USA. *Journal of Glaciology*, 52(177):251-256.

Grove, J. M. 1988. *The Little Ice Age*. London, Routledge. 498 p.

Haeberli, W. 1995. Glacier fluctuations and climate change detection--Operational elements of a worldwide monitoring strategy. *Bulletin, World Meteorological Organization*, 44(1):23-31.

Hall, M. H. and Fagre, D. B. 2003. Modeled Climate-Induced Glacier Change in Glacier National Park, 1850-2100. *BioScience*, 33(2):131-140.

Harrison, A. E. 1956. Glacial activity in the western United States. *Journal of Glaciology*, 2(19):666-668.

Harrison, A. E. 1960. *Exploring Glaciers-with a Camera.* San Francisco, CA, Sierra Club Books. 71 p.

Harwell, C. A. 1931. Yosemite National Park Report on Glacier Surveys:1931 Report. Yosemite National Park. 28 p.

Heald, W. F. 1947. Palisade Glacier survey, Sierra Nevada. *American Alpine Journal*, 6(3):332-339.

Heermance, R. V. and Briggs, R. 2005. Recession of modern glaciers and post-last glacial maximum glacial chronology in the Trinity Alps, CA,. *Abstracts with Programs-Geological Society of America*, 37.

Hoelzle, M., Chinn, T., Stumm, D., Paul, F., Zemp, M. and Haeberli, W. 2007. The application of glacier inventory data for estimating past climate change effects on mountain glaciers: A comparison between the European Alps and the Southern Alps of New Zealand. *Global and Planetary Change. Climate Change Impacts on Mountain Glaciers and Permafrost*, 56(1-2):69-82.

Hoffman, M. J., Fountain, A. G. and Achuff, J. M. 2007. Twentieth-century variations in area of small glaciers and icefields, Rocky Mountain National Park, Rocky Mountains, Colorado, USA. *Annals of Glaciology*, 46.

Howat, I. M. and Tulaczyk, S. 2005. Trends in spring snowpack over a half-century of climate warming in California, USA. *Annals of Glaciology*, 40:151-156.

Howat, I. M., Tulaczyk, S., Rhodes, P., Israel, K. and Snyder, M. 2007. A precipitation-dominated, mid-latitude glacier system: Mount Shasta, California. *Climate Dynamics*, 28(1):85-98.

Hubbard, D. H. 1954. Report of Glacier Studies in Yosemite National Park: 1954 Report. Yosemite National Park. 39 p.

Hubley, R. C. 1956. Glaciers of the Washington Cascades and Olympic Mountains; their present activity and its relation to local climatic trends. *Journal of Glaciology*, 2(19):669-674.

Jackson, K. M. and Fountain, A. G. 2007. Spatial and morphological change on Eliot Glacier, Mount Hood, Oregon, USA. *Annals of Glaciology*, 46:222-226.

Jones, P. D., Osborn, T. J. and Briffa, K. R. 2001. The Evolution of Climate Over the Last Millennium. *Science*, 292(5517):662-667.

Kehrlein, O. 1948. California's Frozen Water Supply. *Pacific Discovery*, 1(4):18-25.

Key, C. H., Fagre, D. B. and Menicke, R. K. 1998. Glacier retreat in Glacier National Park, Montana. *Satellite Image Atlas of Glaciers of the World, Chapter J, Glaciers of North America. U.S. Geological Survey Professional Paper 13686-J.* R. S. Williams and J. G. Ferrigno: 365-375 p.

King, C. 1871. On the Discovery of actual Glaciers on the Mountains of the Pacific Slope. *American Journal of Science and Arts*, Third Series, i:157-167.

Klett, M., Manchester, E., Verburg, J., Bushaw, G. and Dingus, R. 1984. *Second View: The Rephotographic Survey Project. Essay by Paul Berger.* Albuquerque, University of New Mexico Press. 224 p.

Konrad, S. K. and Humphrey, N. F. 2000. Steady-state flow model of debris-covered glaciers (rock glaciers). *In: Debris-Covered Glaciers*. IAHS Publication no. 264: 255-263 p.

Kuhn, I. M. 1995. The mass balance of very small Glaciers. *Zeitschrift für Gletscherkunde und Glazialgeologie, Band*, 31(S):171-179.

LaChapelle, E. R. 1965. The mass budget of Blue Glacier, Washington. *Journal of Glaciology*, 5(41):609-623.

LeConte, J. 1873. On some of the ancient Glaciers of the Sierras. *American Journal of Science and Arts*, Third Series, v:325-342.

López-Moreno, J. I., Nogués-Bravo, D., Chueca-Cía, J. and Julián-Andrés, A. 2006. Glacier development and topographic context. *Earth Surface Processes and Landforms*, 31(12):1585-1594.

Major, J. 1990. California climate in relation to vegetation. *Terrestrial Vegetation of California. Special publication no. 9,*. M. G. Barbour and J. Major. University of California, Davis, California Native Plant Society Press: 11-74 p.

Mantua, N. J., Hare, S. R., Zhang, Y., Wallace, J. M. and Francis, R. C. 1997. A Pacific interdecadal climate oscillation with impacts on salmon production. *Bulletin of the American Meteorological Society*, 78:1069-1079.

Matthes, F. E. 1939. Report of the Committee on Glaciers. *Transactions of the American Geophysical Union*:518-523.

Matthes, F. E. 1940. Committee on glaciers, 1939-1940. *Transaction, American Geophysical Union*:396-406.

McClung, D. and Schaerer, P. 2006. *The Avalanche Handbook*. Seattle, The Mountaineers Books. 342 p.

Meier, M. F. 1961. Distribution and Variations of Glaciers in the United States Exclusive of Alaska. *General Assembly of Helsinki, July 25-August 6, 1960: Commission of Snow and Ice: Gentbrugge*, 54:420-429.

Meier, M. F. 1965. Glaciers and climate. *The Quaternary of the United States*. H. E. Wright and F. D.G. Princeton, N.J., Princeton University Press: 795-805 p.

Meier, M. F., Dyurgerov, M. B., Rick, U. K., O'Neel, S., Pfeffer, W. T., Anderson, R. S., Anderson, S. P. and Glazovsky, A. F. 2007. Glaciers Dominate Eustatic Sea-Level Rise in the 21st Century. *Science*, 317(5841):1064-1067.

Millar, C. I., Westfall, R. D., Delany, D. L., King, J. C. and Granumlich, L. J. 2004. Response of subalpine conifers in the Sierra Nevada, California, U.S.A., to twentieth-century warming and decadal climate variability. *Arctic, Antarctic, and Alpine Research*, 36(2):181-200.

Mote, P. W., Hamlet, A. F., Clark, M. P. and Lettenmaier, D. P. 2005. Declining mountain snowpack in western North America. *Bulletin of the American Meteorological Society*, 86(1):39-49.

Muir, J. 1873. On Actual Glaciers in California. *American Journal of Science and Arts*, Third Series, v:69-71.

Mutch, L., Rose, M., Heard, A., Cook, R. R. and Entsminger, G. 2006. Vital Signs Monitoring Plan, Phase III Draft Report, Sierra Nevada Network, National Park Service.

NCDC 2002. Monthly Normals of Temperature, Precipitation, and Heating and Cooling Degree Days 1971-2000: California. Asheville, North Carolina, National Climatic Data Center/NESDIS/NOAA. 73 p.

NCDC 2006. Climate of the States: California. Climatography of the United States NO. 60, NOAA, Available:http://hurricane.ncdc.noaa.gov/cgi-bin/climatenormals.

NOAA 2006. Oceanic Nino Index 1951 - present. Climate Prediction Center, Available:http://www.cpc.noaa.gov/products/analysis_monitoring/ensostuff.

Nylen, T. 2004. Spatial and Temporal Variations of Glaciers on Mount Rainier between 1913 and 1994. Masters Thesis, Department of Geology, Portland State University, Portland, OR: 94 p.

Oerlemans, J. 2005. Extracting a Climate Signal from 169 Glaciers. *Science*, 308(5722):675-678.

Paterson, W. S. B. 1999. *The Physics of Glaciers*. Tarrytown, N.Y., Pergamon. 496 p.

Porter, S. C. 1981. Glaciological evidence of Holocene climatic change. *Climate and History*. T. M. L. Wigley, M. J. Ingram and C. Fermer. Cambridge, Cambridge University Press: 82-110 p.

Post, A., Richardson, D., Tangborn, W. V. and Rosselot, F. L. 1971. Inventory of Glaciers in the North Cascades, Washington. *USGS Prof. Pap. 705-A*.

Raub, W. B., Brown, C. S. and Post, A. 2006. Inventory of Glaciers in the Sierra Nevada, California, US Geological Survey Open-File Report 2006-1239. 232 p.

Rhodes, P. 1987. Historic Glacier Fluctuations at Mount Shasta. *California Geology*, 40(9):205-209.

Russell, I. C. 1885. Existing Glaciers of the United States. 5th Annual Report of the U.S. Geologic Survey, 1883-84. 303-355 p.

Russell, I. C. 1889. Quaternary history of Mono Valley, California. 8th Annual Report of the U.S. Geologic Survey, 1886-67. 261-394 p.

Stewart, I. T., Cayan, D. R. and Dettinger, M. D. 2005. Changes towards earlier streamflow timing across Western North America. *Journal of Climate*, 18:1136-1155.

Stine, S. 1996. Climate of the Sierra Nevada, 1650-1850. Chapter 2. *Sierra Nevada Ecosystem Project: Final Report to Congress: Assessments and Scientific Basis for Management Options*. II: 25-30 p.

Tangborn, W. V., Fountain, A. G. and Sikonia, W. G. 1990. Effect of Area Distribution with Altitude on Glacier Mass Balance - A comparison of North and South Klawatti Glaciers, Washington State, U.S.A. *Annals of Glaciology*, 14:278-282.

Tangborn, W. V., Mayo, L. R., Scully, D. R. and Krimmel, R. M. 1977. Combined ice and water balances of Maclure Glacier, California, South Cascade Glacier, Washington, and Wolverine and Gulkana Glaciers, Alaska, 1967 Hydrologic Year: U.S. Geological Survey Prof. Paper 715- B. 20 p.

Trenberth, K. E., Jones, P. D., Ambenje, P., Bojariu, R., Easterling, D., Klein Tank, A., Parker, D., Rahimzadeh, F., Renwick, J. A., Rusticucci, M., Soden, B. and Zhai, P. 2007. Observations: Surface and Atmospheric Climate Change. In: Climate Change 2007: The Physical Science Basis. Contribution of Working Group I to the Fourth Assessment Report of the Intergovernmental Panel on Climate Change, Cambridge University Press, Cambridge, United Kingdom and New York, NY, USA. p.

USGS 1999. Map accuracy standards: U.S. Geological Survey Fact Sheet 171–99. 2 p.

USGS 2006. USGS Photographic Library Archive. United States Geologic Survey, Available:http://libraryphoto.er.usgs.gov/.

White, W. 1976. Report of Glacier Studies in Yosemite National Park: 1975 Report, Yosemite National Park. 20 p.

YOSE 1960. Report of Glacier Studies in Yosemite National Park, 1960 Report. Yosemite National Park. 18 p.

Appendix A. USGS Maps with Glaciers

Compilation of USGS topographic quadrangle maps (1:24,000) that contain glacier and snow features with USGS numerical map ID, Quadrangle name, and year of aerial photographs.

USGS ID	Name	Photo Year
36118-D5	Mineral King	1976, 1983
36118-E3	Mount Whitney	1976, 1978
36118-E4	Mount Kaweah	1976, 1978
36118-E5	Triple Divide Peak	1976, 1978
36118-F3	Mount Williamson	1976, 1978
36118-F4	Mount Brewer	1976, 1978
36118-F5	Sphinx Lakes	1976, 1983, 1984
36118-F6	Mount Silliman	1976, 1983
36118-G3	Kearsarge Peak	1976
36118-G4	Mount Clarence King	1976, 1978
36118-G6	Cedar Grove	1976, 1983
36118-H3	Aberdeen	1976, 1978
36118-H4	Mount Pinchot	1976, 1978
36118-H5	Marion Peak	1984
36118-H6	Slide Bluffs	1976, 1983
37118-A4	Split Mountain	1975, 1979
37118-A5	North Palisade	1976
37118-A6	Mount Goddard	1976
37118-A7	Blackcap Mountain	1976
37118-B5	Mount Thompson	1976
37118-B6	Mount Darwin	1976
37118-B6	Mount Darwin	1976
37118-B7	Mount Henry	1976
37118-C6	Mount Tom	1976
37118-C7	Mount Hilgard	1976
37118-C8	Florence Lake	1976
37118-D6	Mount Morgau	1976
37118-D7	Mount Abbot	1976
37118-D8	Graveyard Peak	1976
37118-E8	Bloody Mountain	1976, 1979
37119-E1	Crystal Crag	1972, 1975, 1979
37119-E2	Cattle Mountain	1975, 1976
37119-F2	Mount Ritter	1975, 1976
37119-F3	Mount Lyell	1984, 1985
37119-F4	Merced Peak	1984, 1985
37119-G2	Koip Peak	1975, 1982, 1984
37119-G3	Vogelsang Peak	1984, 1985
37119-G4	Tenaya Lake	1984, 1985
37119-H2	Mount Dana	1975, 1982, 1984
37119-H3	Tioga Pass	1984
38119-A2	Lundy	1982

USGS ID	Name	Photo Year
38119-A3	Dunderberg Peak	1984, 1985
38119-A4	Matterhorn Peak	1984, 1985
38119-A5	Piute Mountain	1984
38119-B4	Buckeye Ridge	1975, 1982, 1984
38119-B5	Tower Peak	1984
38119-B6	Emigrant Lake	1984
38119-C5	Pickel Meadow	1953
38119-C6	Sonora Pass	1973

Appendix B. Repeat Photography

Dates and locations of repeat photographs. Locations are provided in WGS 1984 coordinate system.

Glacier	Photographer	Original date	Repeat date	Latitude	Longitude
Goddard Glacier	G.K. Gilbert	Aug-13-1908	Aug-16-2004	37.125021	-118.703488
Darwin Glacier	G.K. Gilbert	Aug-14-1908	Aug-14-2004	37.175947	-118.670484
Lyell Glacier	G.K. Gilbert	Aug-07-1903	Sep-05-2004	37.753291	-119.274928
Maclure Glacier	G.K. Gilbert	Aug-07-1903	Aug-14-2003	37.757554	-119.279845
Dana Glacier	I.C. Russell	1883	Sep-08-2004	37.910503	-119.221634
Conness Glacier	G.K. Gilbert	1903	Sep-23-2004	37.966961	-119.321251

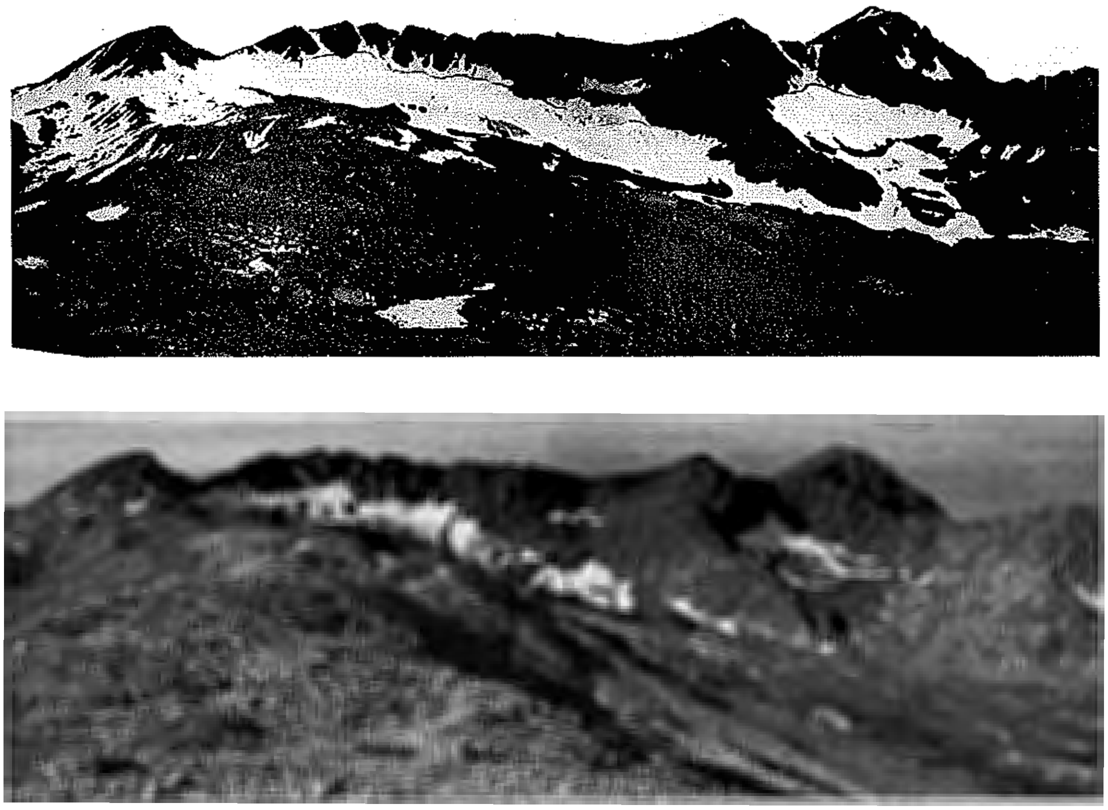

Appendix-B1. Goddard Glacier, Kings Canyon National Park. Top photo taken on August 13, 1908 by G.K. Gilbert (USGS Photographic Library), bottom photo taken on August 16, 2004 by Hassan Basagic.

Appendix-B2. Darwin Glacier, Kings Canyon National Park. Top photograph taken on August 14, 1908 by G.K. Gilbert (USGS Photographic Library), bottom photograph by Hassan Basagic, August 14, 2004.

Appendix-B3. The East (left) and West (right) lobes of Lyell Glacier. Top photo by G.K. Gilbert, August 7, 1903 (USGS Photographic Library), bottom photo taken on September 5, 2004 by Hassan Basagic.

Appendix-B4. Maclure Glacier, Yosemite National Park, Top photograph by G.K. Gilbert, August 7, 1903. USGS Online Photographic Archive), bottom photograph taken on August 14, 2003, by Hassan Basagic.

Appendix-B5. Dana Glacier, top photo taken in 1883 by I.C. Russell, bottom photo taken on September 8, 2004 by Hassan Basagic.

Appendix-B6. Conness Glacier, top photo taken in 1903 by G.K. Gilbert; bottom photo taken on September 23, 2004 by Hassan Basagic.

Appendix C. Glacier Change Metadata

Compilation data of each year depicted for 14 glaciers. Type key: AP-aerial photograph, GPS-Global Positioning System field mapping, TGP-terrestrial ground photo. Sources key: YOSE-Yosemite National Park Archive, USFS-US Forest Service Bishop Office Archive, SEKI-Sequoia & Kings Canyon National Parks Archive, NAIP-National Agriculture Imagery Program. Also included are glacier areas with root mean square errors (RMSE) for georeferenced aerial photographs and GPS error and associated error.

Glacier	Year	Data	Date	Source	Area (km^2)	RMSE (m)	Inner error (km^2)	Outer error (km^2)
Dragontooth	1900	moraine	N/A	geologic	0.2094	10.0	0.0257	0.0264
Dragontooth	2006	AP / TGP	2005 / 2006	NAIP / Basagic	0.0548	7.0	0.0123	0.013
Conness	1900	moraine	N/A	geologic	0.3339	4.9	0.0119	0.0121
Conness	1944	AP	9/27/1944	YOSE	0.2611	4.9	0.0101	0.0102
Conness	1954	AP	8/19/1954	USFS	0.2304	5.9	0.0116	0.0118
Conness	1972	AP	8/14/1972	USFS	0.1977	9.9	0.0193	0.0199
Conness	2004	GPS	9/23/2004	Basagic	0.1600	2.5	0.0044	0.0044
Dana	1900	moraine	N/A	geologic	0.3193	10.0	0.0294	0.0300
Dana	2003	GPS	8/18/2003	Basagic	0.1153	5.0	0.0116	0.0167
Maclure	1900	moraine	N/A	geologic	0.2930	10.0	0.0234	0.0241
Maclure	2003	GPS	8/7/2003	Basagic	0.1553	5.0	0.0089	0.0090
West Lyell	1900	moraine	N/A	geologic	0.4643	10.0	0.0331	0.0339
West Lyell	1916	TGP	8/14/1916	unknown	0.4643	10.0	0.0331	0.0339
West Lyell	1931	TGP	10/1/1931	NPS, 1931	0.4329	11.2	0.0377	0.0382
West Lyell	1944	AP	9/28/1944	YOSE	0.4088	11.2	0.0235	0.0239
West Lyell	1955	AP	8/8/1955	YOSE	0.3417	6.9	0.0184	0.0189
West Lyell	1972	AP	8/14/1972	USFS	0.3233	8.0	0.0209	0.0215
West Lyell	2003	GPS	8/13/2003	Basagic	0.2970	5.0	0.0132	0.0134
West Lyell	2004	GPS	9/3/2004	Basagic	0.2795	2.5	0.0063	0.0063

Glacier	Year	Data	Date	Source	Area (km^2)	RMSE (m)	Inner error (km^2)	Outer error (km^2)
East Lyell	1900	moraine	N/A	geologic	0.6334	10.0	0.0495	0.0487
East Lyell	1903	TGP	8/7/1904	Gilbert	0.6189	10.0	0.0495	0.0487
East Lyell	1914	TGP	3/28/1905	Matthes	0.6189	10.0	0.0495	0.0487
East Lyell	1923	TGP	9/13/1923	YOSE	0.5451	10.0	0.0335	0.0154
East Lyell	1931	TGP	10/1/1931	NPS, 1931	0.4908	11.2	0.0393	0.0401
East Lyell	1944	AP	9/28/1944	YOSE	0.3821	11.2	0.0456	0.0463
East Lyell	1955	AP	8/8/1955	YOSE	0.3174	12.1	0.0437	0.0452
East Lyell	1960	TGP	9/9/1960	NPS, 1960	0.3001	10.0	0.034	0.0346
East Lyell	1972	AP	8/14/1972	USFS	0.2621	9.0	0.0301	0.0306
East Lyell	1987	TGP	9/14/1987	YOSE, D. Hardy	0.2691	20.0	0.0728	0.0683
East Lyell	2003	GPS	8/13/2003	Basagic	0.1855	5.0	0.0196	0.0197
East Lyell	2004	GPS	9/2/2004	Basagic	0.1402	2.5	0.0089	0.0089
Darwin	1900	moraine	N/A	geologic	0.2536	10.0	0.0265	0.0271
Darwin	1908	TGP	8/14/1908	Gilbert	0.2536	10.0	0.0265	0.0271
Darwin	1948	AP	10/7/1948	USFS	0.1419	5.5	0.0116	0.0118
Darwin	1973	AP	9/9/1973	SEKI	0.1226	5.2	0.0108	0.0110
Darwin	2001	AP	7/29/2001	SEKI	0.1345	6.0	0.0067	0.0067
Darwin	2004	GPS	8/12/2004	Basagic	0.1172	2.5	0.0055	0.0056
Goddard	1900	moraine	N/A	geologic	0.3787	10.0	0.0333	0.0343
Goddard	1908	TGP	8/15/1908	Gilbert	0.3787	10.0	0.0333	0.0343
Goddard	1948	AP	10/7/1948	USFS	0.2566	7.2	0.0224	0.0228
Goddard	1973	AP	9/8/1973	SEKI	0.2051	3.5	0.0110	0.0110
Goddard	2004	GPS	8/15/2004	Basagic	0.1734	2.5	0.0092	0.0092
Middle Goddard	1900	moraine	N/A	geologic	0.1106	10.0	0.0148	0.0154
Middle Goddard	2004	GPS	8/15/2004	Basagic	0.0347	2.5	0.0028	0.0028
Black Giant	1900	moraine	N/A	geologic	0.1120	10.0	0.0149	0.0154
Black Giant	2004	GPS	8/17/2004	Basagic	0.0688	5.0	0.0073	0.0075
Middle Palisade	1900	moraine	N/A	geologic	0.3071	10	0.0232	0.0239
Middle Palisade	2005	AP	2005	NAIP	0.1735	7	0.014	0.0143

Glacier	Year	Data	Date	Source	Area (km^2)	RMSE (m)	Inner error (km^2)	Outer error (km^2)
Brewer	1900	moraine	N/A	geologic	0.1456	10.0	0.0161	0.0168
Brewer	2005	AP	2005	NAIP	0.0418	7.0	0.0081	0.0084
Lilliput	1900	moraine	N/A	geologic	0.0699	10.0	0.0112	0.0118
Lilliput	1973	AP	9/9/1973	SEKI	0.0521	5.2	0.0059	0.0061
Lilliput	2001	AP	7/29/2001	SEKI	0.0559	3.0	0.0034	0.0033
Lilliput	2004	GPS	7/30/2004	Basagic	0.0485	2.5	0.0029	0.0029
Picket	1900	moraine	N/A	geologic	0.1555	10.0	0.0157	0.0163
Picket	1973	AP	8/29/1973	SEKI	0.1041	4.1	0.0058	0.0059
Picket	2004	GPS	8/27/2004	Basagic	0.0798	2.5	0.0032	0.0033

Appendix D. Rates of Glacier Area Change for Seven Glaciers.

Glacier	Years	Area change (m^2)	Number of Years	Rate of change (m2 yr^{-1})
Conness	1900 - 1944	-72784	44	-1654
	1944 - 1954	-30633	10	-3063
	1954 - 1972	-32760	18	-1820
	1972 - 2004	-37708	32	-1178
West Lyell	1900 - 1903	0	3	0
	1903 - 1916	0	13	0
	1916 - 1931	-31440	15	-2096
	1931 - 1944	-24072	13	-1852
	1944 - 1955	-67153	11	-6105
	1955 - 1972	-18428	17	-1084
	1972 - 2003	-26252	31	-847
	2003 - 2004	-17510	1	-17510
East Lyell	1900 - 1903	0	3	0
	1903 - 1914	0	11	0
	1914 - 1923	-64859	9	-7207
	1923 - 1931	-58275	8	-7284
	1931 - 1944	-108684	13	-8360
	1944 - 1955	-64734	11	-5885
	1955 - 1960	-17301	5	-3460
	1960 - 1972	-37958	12	-3163
	1972 - 1987	6952	15	463
	1987 - 2004	-128915	17	-7583
Darwin	1900 - 1908	0	8	0
	1908 - 1948	-111780	40	-2795
	1948 - 1973	-19277	25	-771
	1973 - 2001	11899	28	425
	2001 - 2004	-17317	3	-5772
Goodard	1900 - 1908	0	8	0
	1908 - 1948	-122104	40	-3053
	1948 - 1973	-51486	25	-2059
	1973 - 2004	-31680	31	-1022
Picket	1900 - 1973	-51469	73	-705
	1973 - 2004	-24245	31	-782
Lilliput	1900 - 1973	-17838	73	-244
	1973 - 2001	3830	28	137
	2001 - 2004	-7418	3	-2473

Appendix E. Glacier Area Change Maps and Area-Altitude Distributions for Seven Study Glaciers

Maps of spatial changes were created for each of the seven study glaciers (Appendix E1 and E2). Area-altitude distributions were also created of each of the seven glaciers for the 1900 and 2004 boundaries (Appendix E3). Area-altitude differences can be important to understanding how a glacier responds to climate variations (Tangborn et al., 1990). The area-altitude distributions for the seven glaciers are based on a 10-meter DEM derived from the original USGS topographic maps from 1976 – 1984. These elevations are approximate and used here for general comparison. Based on my examination of historic photographs, the area in the lower portions of the 1900 area-altitude distributions would likely be 10 to 20 m higher than depicted.

The most dramatic change amongst the glaciers occurred at Lyell Glacier. In 1900 the two lobes were connected by an icefall and at the glacier terminus, when the area-altitude distributions of the two lobes were differed. East Lyell Glacier contained more area in the lower elevations (3550 – 3750m) compared to the upper portion of the glacier (3750 – 3900m). In contrast, West Lyell Glacier was fairly evenly distributed thorough out (3650 – 3950m). By 2004 East Lyell Glacier had receded to elevations above 3600 m with some loss in the upper reaches. The West Lyell Glacier lost all area below 3650m. Because of the extensive low lying glacier elevations of East Lyell Glacier, it lost a greater area than West Lyell Glacier. Area losses at Conness, Picket, and Lilliput glaciers were similar, with losses occurring in the lowest elevations. In contrast, the area change at Darwin Glacier was proportional over all elevations caused recession of the northern portion of the glacier.

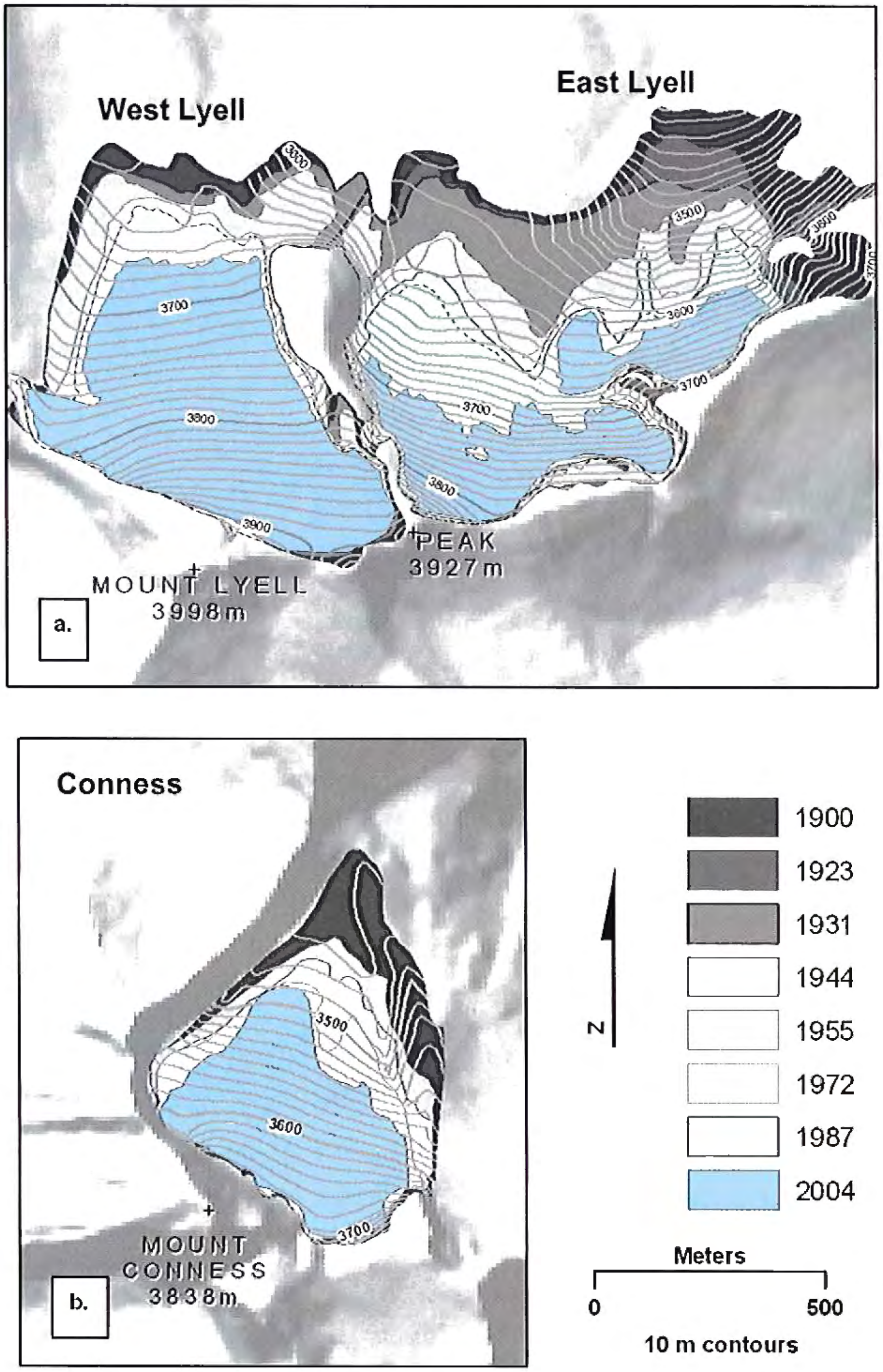

Appendix E1. Individual glacier chronology maps for (a) West and East Lyell Glacier, and (b) Conness Glacier. The 1973 boundary of Lyell Glacier is dashed where the glacier was smaller than the 1987 extent.

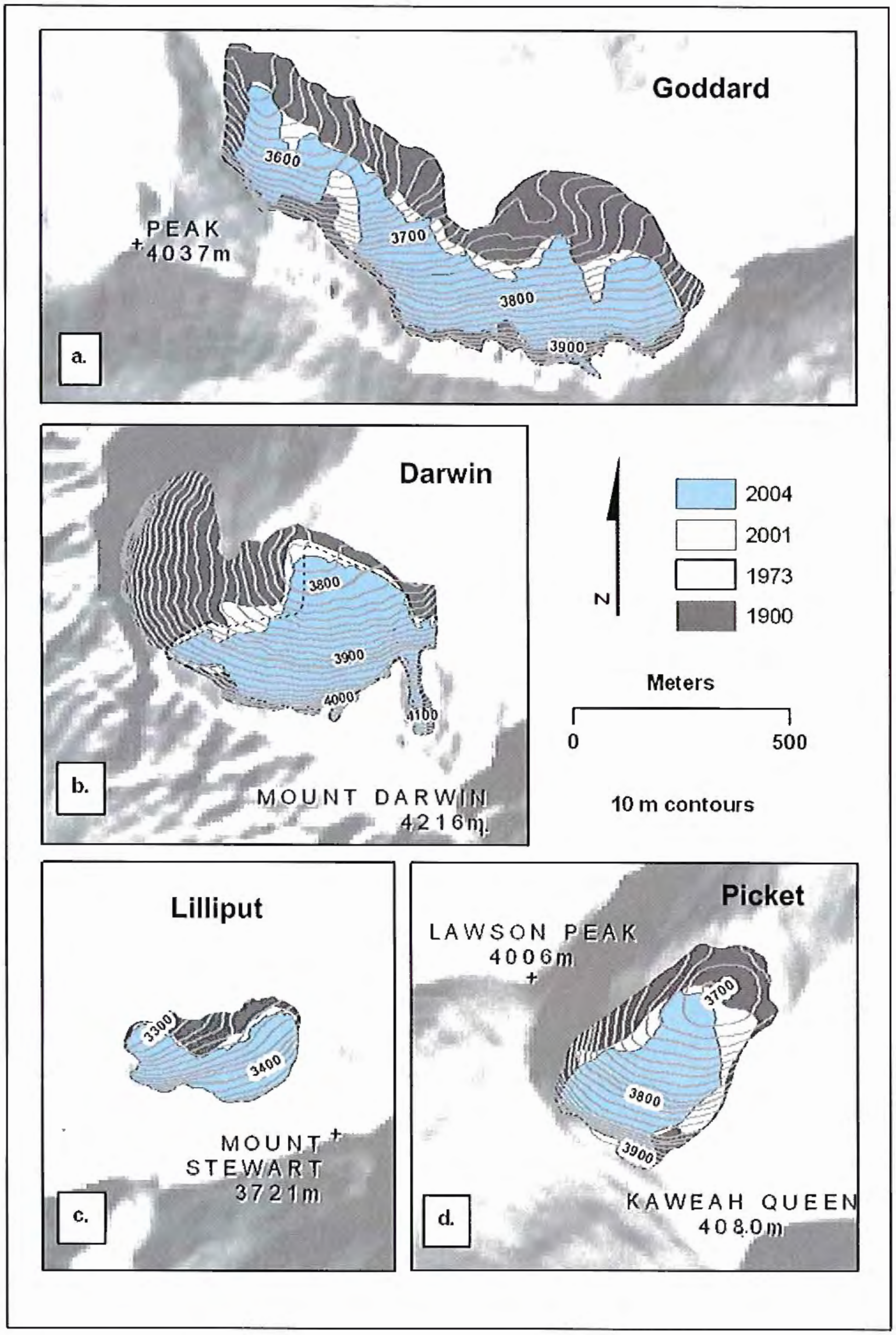

Appendix E2. Individual glacier chronology maps for (a) Goddard Glacier, (b) Darwin Glacier, (c) Lilliput Glacier, and (d) Picket Glacier. The 1973 boundary of Darwin Glacier is dashed where the glacier was smaller than the recent extents.

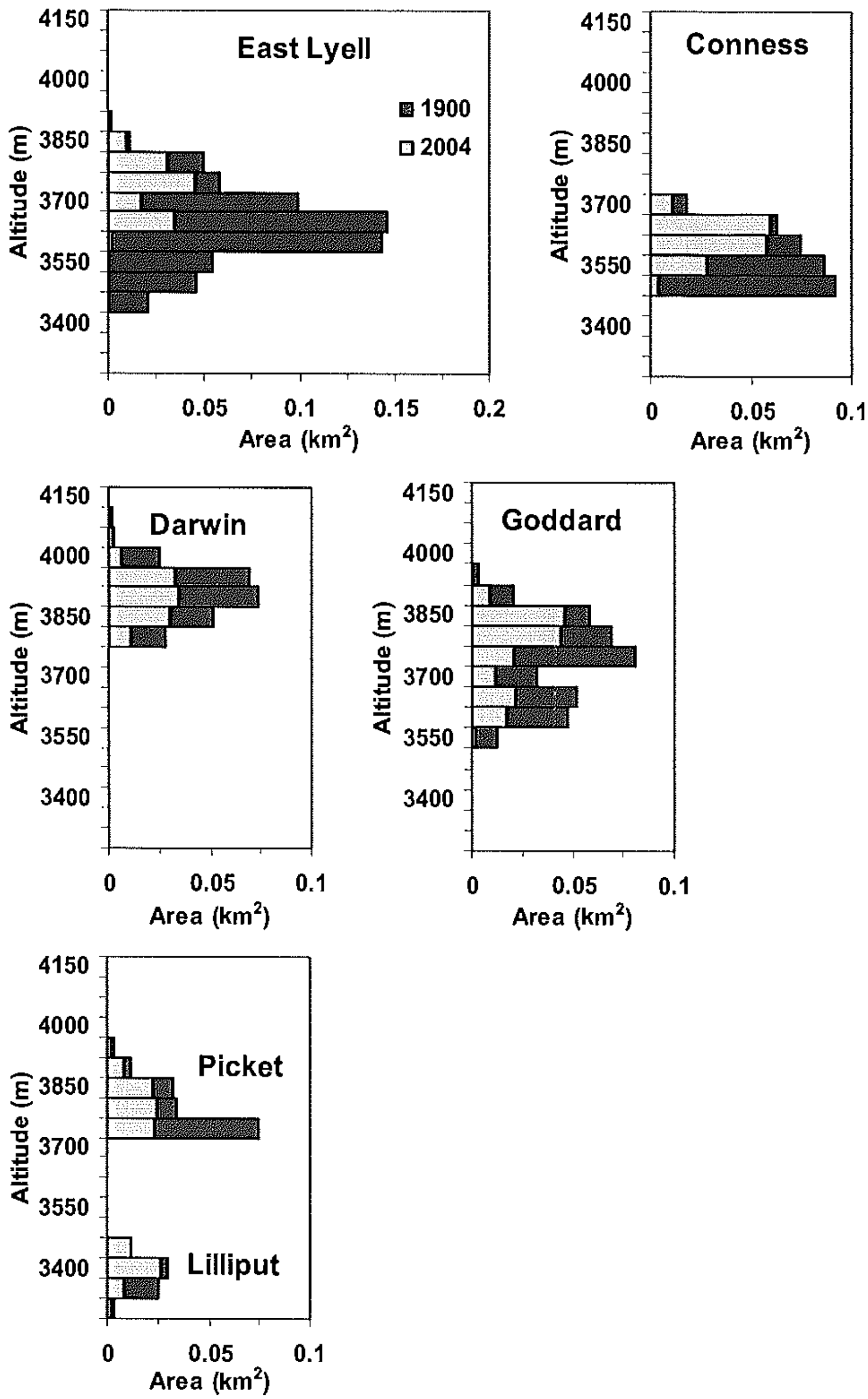

Appendix E3. Area-altitude distributions at seven glaciers in 1900 (grey) and 2004 (dark grey) using 50m size intervals.